Structure, Dynamics, and Spectroscopy of Aniline−(Argon)$_n$ Clusters. 1. Experimental Spectra and Interpretation for $n = 1-6$

S. Douin,[†] P. Parneix,[†] F. G. Amar,[‡] and Ph. Bréchignac*,[†]

Laboratoire de Photophysique Moléculaire, CNRS, Université de Paris-Sud, Bâtiment 213, 91405 Orsay Cedex, France, and Department of Chemistry, University of Maine Orono, Maine 04469

Received: February 29, 1996; In Final Form: October 22, 1996[⊗]

An experimental spectroscopic study of the van der Waals aniline−Ar$_n$ clusters ($n = 1-6$) has been achieved via resonant two-photon two-color ionization, whose results improve the accuracy of the previously reported spectra and complete them by the observation of further structure in the spectra of well-defined structural isomers. These experimental results have been analyzed in detail in relation with molecular dynamics simulations including minimum energy structures calculations, direct spectral simulations, and isomerization dynamics. Two potential energy surfaces, in both the ground S_0 and the electronically excited S_1 states, have been built in order to recover the main experimental observables. They permit the site specific electronic shift additivity rule to be confirmed by the semiclassical spectral simulations and a global picture of the solvation phenomena in this aromatic−rare gas atom system to be provided. In particular, careful examination of the isomerization dynamics helps the general understanding of the structural behavior of these microsolvent clusters.

1. Introduction

During the last decade, van der Waals clusters consisting of a solute molecule embedded in a cluster of solvent molecules have been recognized as a powerful tool for investigating the intimate mechanisms of the solvation process.[1,2] Among the various kinds of microsolvent clusters which have been thoroughly studied, those using an aromatic molecule as the solute carrying the oscillator strength for optical excitation are many,[3−9] probably because they are well suited for experimental interrogation by resonant two-photon ionization (R2PI), which is able to provide the size selection. The influence of the solvent on the spectroscopic properties of the chromophore is often a major goal of the studies. The most common observables are the spectroscopic shifts of the first allowed electronic transition and of the ionization potential.[6,10−14] The assignment of spectral bands to specific isomers of a given cluster size is a recent development.[6,9,15−17]

An alternative approach is to investigate the dynamical behavior of these weakly bound systems and more specifically to understand the redistribution of vibrational energy in the intermolecular modes. In that approach, the use of theoretical tools like quantum mechanical methods to derive bound states energies and wavefunctions[18−23] and/or classical numerical simulations methods to explore real time (molecular dynamics)[17,24−27] or random-walk (Monte-Carlo) trajectories[28−30] has proven to be very powerful. As a matter of fact experimental information on this dynamics is accessible through the analysis of the spectra of size-selected clusters. Most importantly, analysis of vibrationally excited van der Waals modes and of the shifts and shapes of the bands is very useful.

A number of studies of the microsolvation of aromatic molecules have made use of argon (or another noble gas) as an inert solvent and have been concerned with the problem of discriminating the possible spectral signatures of intracluster phase transitions versus the blending of spectral features originating from a population of different structural isomers. The benzene/argon system, which could have been considered as a paradigm, turned out to be much more specific than expected.[3,5,20,31] Surprising van der Waals induced vibronic couplings have been finally recognized after a period when the proper assignments of the van der Waals modes in the 1:1 cluster remained puzzling.[21] Two main classes of structural isomers were then proposed to explain the spectra of larger clusters.[29]

More classical behaviors were characterized in other solute/solvent systems, like napthalene/argon,[6] carbazole/argon,[32] 9,10-dichloroanthracene/krypton (argon),[7] and 1,2-dimethylnaphthalene/argon.[8] They have revealed the appearance of so-called wetting versus nonwetting structures as a function of cluster size. In the case of carbazole/argon,[12,33] rigid and fluxional families of isomers have been spectroscopically separated in an elegant way thanks to a propitious shift of the ionization potential.

The present paper is the first of two articles (referred as to 1 and 2) devoted to a detailed investigation, both experimental and theoretical, of the aniline/argon solute/solvent system, which emphasizes the analysis of internal dynamics through the use of extensive numerical simulations. The spectroscopic specificity of the aniline molecule in its first allowed electronic transition is due to the transfer of electron density from the lone pair orbital on nitrogen to the π orbital of the phenyl ring upon electronic excitation. This has been recognized as the main cause for the *blue* spectral shifts observed when argon atoms lying in the vicinity of the nitrogen atom interact efficiently with the concerned orbital. It will be shown in the body of this work that this feature is essential to account for the nonstandard spectral behavior which was obtained in that system. The goal of the whole work is to provide a presentation and discussion of all experimental as well as theoretical results in a consistent way. Paper 1 focuses on the smaller aniline−Ar$_n$ cluster sizes ($n = 1-6$), while paper 2 will be devoted to the larger sizes ($n = 7-25$).

* Author to whom correspondence is to be addressed. E-mail address: phb@psisun.u-psud.fr. Fax number: 33-1-69-41-67-77.

[†] Université de Paris-Sud. Laboratoire associé à l'Université de Paris-Sud.

[‡] University of Maine.

[⊗] Abstract published in *Advance ACS Abstracts,* December 15, 1996.

S1089-5639(96)00620-2 CCC: $14.00

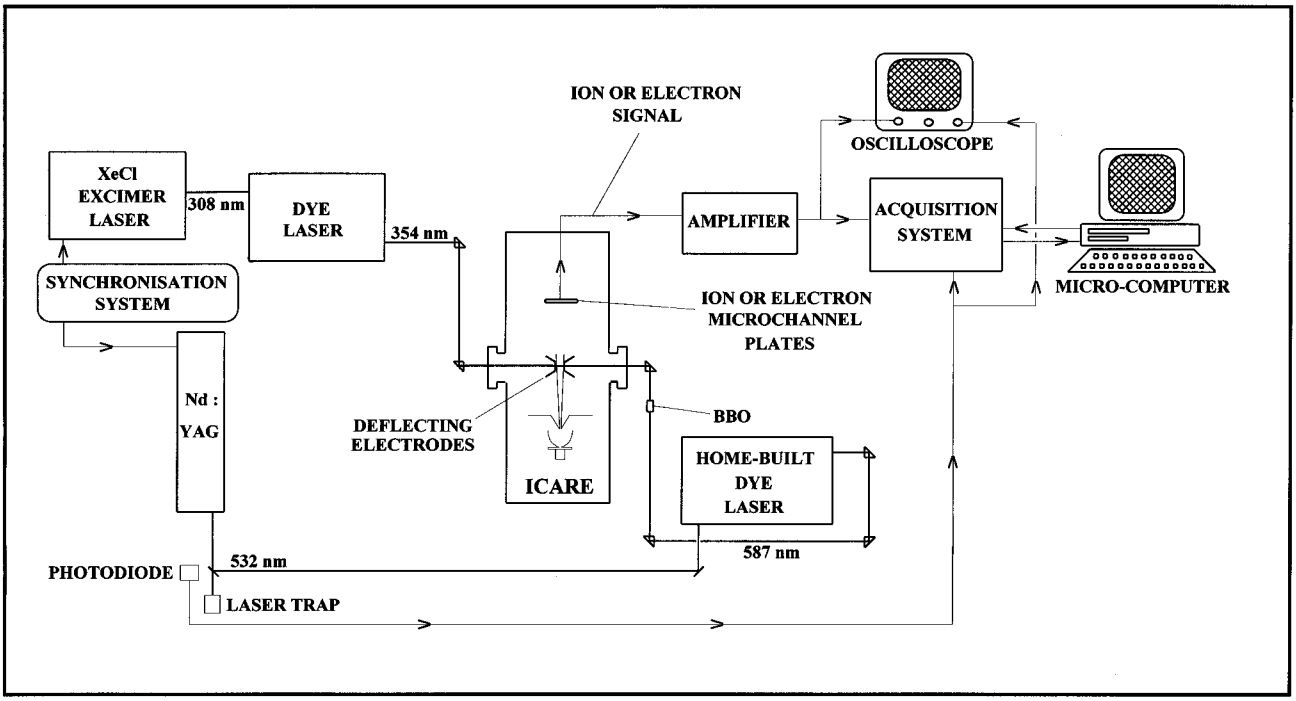

Figure 1. Block diagram of the "ICARE" experimental setup.

The outline of the present article is as follows: the next two sections present the methodology, both experimental (section 2) and theoretical (section 3), including the techniques used to characterize the isomerization dynamics and to simulate electronic spectra. Section 4 describes and discusses the results by order of increasing size.

2. Experimental Section

The experimental apparatus, called *ICARE*, has been already described in a previous publication.[34] Briefly, it consists of a dual time-of-flight photoelectron (commercial magnetic bottle)[35] and photoion (home-built) spectrometer, adapted to a pulsed supersonic molecular beam apparatus. The very efficient rotational cooling of the beam (about 0.5 K) permits the formation of van der Waals (vdW) clusters, such as aniline−Ar$_n$. These clusters are generated by expanding an aniline:Ar:He gas mixture through a circular nozzle (750 μm in diameter) into the first vacuum chamber of the apparatus.

Resonant two-photon two-color ionization (R2P2CI) was used to ionize the aniline molecule and its clusters with argon. In this technique, one photon of the first color is used to excite the aniline molecule from its ground state to its first electronically excited state S_1, and quasi-simultaneously (within a lifetime), a photon from the second laser ionizes the molecule. The advantage of this two-color technique is to allow ionization of the species with a photon energy which is very close to the ionization threshold and thus, in the case of vdW clusters, to minimize the fragmentation which could arise from excess vibrational energy deposited in the ions. By scanning the frequency of the first laser, we are able to record the resonantly enhanced photoionization spectra of size-selected neutral clusters.

Figure 1 is a block diagram of the experimental setup, showing the lasers and the ICARE apparatus. A 532 nm beam originating from a Nd:YAG (Quantel YG481-15) laser, with 70 mJ of energy, was used to pump a home-built dye laser operating with Rhodamine-6G in order to provide a 590 nm beam with 7 mJ of energy. After frequency doubling with a BBO crystal, the resulting UV beam was used to excite the cluster species from the ground state to the first electronically excited state S_1, located at 34 029 cm^{-1} in bare aniline. The 308 nm output beam from a Lambda-Physik EMG 102 MSC laser was used to pump a Lambda-Physik FL2002 dye laser containing DMQ dye delivering a UV beam (around 360 nm) with about 10 mJ of energy. This beam was used to realize the ionization step.

Since the lifetime of the first electronically excited state (8 ns for the monomer) is of the same order of magnitude as the laser pulse duration, it is important to synchronize the two lasers. This has been achieved by a home-built delay line synchronization system. After their superimposition in time was optimized, the two UV beams were sent anticollinearly at right angles to the molecular beam, as shown in Figure 1, and were spatially superimposed.

After ionization of the species, the ion signal was collected onto microchannel plates, displayed on a digital oscilloscope (Lecroy 9420), and stored by the acquisition system after proper gating. To obtain separated spectra for clusters of different sizes, we gated the ion signal on several time windows corresponding to the times of flight in the mass spectrometer of the species of interest while the frequency of the first laser was scanned.

3. Theory

3.A. Methods and Potentials. In this work, the dynamics of the aniline−Ar$_n$ clusters is studied by classical mechanics. To simulate microcanonical trajectories in phase space, we integrate the Newton and Euler−Lagrange equations for translational and rotational motions respectively by using a fifth- and a fourth-order predictor−corrector algorithm with a typical time step equal to 5 fs. The energy conservation is typically equal to 1 part in 10^5. All the simulations have been performed with the total angular momentum equal to zero.

The aniline molecule is considered as a rigid body by making the assumption that the zero-point vibration of the molecule in the ground state does not affect the dynamics of the Ar atoms

around the chromophore. For numerical reasons, the rotation of the aniline molecule is described by means of quaternions.[36]

We briefly describe now the potential model used for the two electronic states of the aniline molecule. As we consider the aniline molecule as a rigid body, we only need to describe the potential energy for the interaction between the argon atoms and the aniline molecule. This potential can be written as the sum of the interaction energy between the aniline molecule and each solvent atom (V_{An-Ar}) and the interaction potential between the solvent atoms (V_{Ar-Ar}). The first contribution is taken as the sum of Lennard-Jones potentials between all of the atoms of aniline and each argon atom, plus an inductive term

$$V_{An-Ar} = V_{atom-atom} + V_{ind} \tag{1}$$

with

$$V_{atom-atom} = \sum_{i=1}^{14}\sum_{j=1}^{n} V(r_{ij}) \tag{2}$$

where

$$V(r_{ij}) = 4\epsilon_{ij}\left(\left(\frac{\sigma_{ij}}{r_{ij}}\right)^{12} - \left(\frac{\sigma_{ij}}{r_{ij}}\right)^{6}\right) \tag{3}$$

The inductive term can be written as

$$V_{ind} = \sum_{j=1}^{n} \vec{\mu}_a \tilde{T}_{aj} \vec{\mu}_j \tag{4}$$

where $\vec{\mu}_a$ is the permanent dipole of the aniline molecule and $\vec{\mu}_j$ is the dipole induced in the Ar atom. This latter is proportional to the electric field ($\vec{\mu}_j$) created by the permanent dipole in the aniline molecule and is given by

$$\vec{\mu}_j = \alpha \vec{E}_j \tag{5}$$

In these calculations, the polarizability of the Ar atom (α) has been taken as equal to 1.63 Å^3. Values of aniline dipole moments ($\vec{\mu}_a$) in the two electronic states are extracted from the work of J. R. Lombardi:[37] $\mu_a(S_0) = 1.53$ D and $\mu_a(S_1) = 2.48$ D.

In the point dipole approximation,[38] the dipole tensor $\tilde{T}_{aj}$ (eq 4) can be written as

$$\tilde{T}_{aj} = [\tilde{I} - 3(\vec{r}_{aj} \cdot \vec{r}_{aj})/r^2_{aj}]/r^3_{aj} \tag{6}$$

where $\vec{r}_{aj}$ is the vector between the jth Ar atom and the center of the permanent dipole in the aniline molecule.

The interaction potential between two Ar atoms is well-known. From the form given by Aziz and Chen,[39] a potential has been fit (for ease of computation) by S. Weerasinghe and F. G. Amar[40] to the simple analytical form

$$V_{Ar-Ar}(r) = \frac{C_6}{r^6} + \frac{C_8}{r^8} + \frac{C_{10}}{r^{10}} + \frac{C_{12}}{r^{12}} \tag{7}$$

Finally, an empirical contribution $V_{:N-Ar}$ to the potential in the S_1 state, already discussed in a previous publication,[23] has been added to describe the *specific* interaction between Ar atoms and the lone pair orbital on the nitrogen atom of the $-NH_2$ group and to account, in particular, for a lowering of the dispersion energy in the S_1 state when the Ar atom is located in a site next to the $-NH_2$ functional group. This term tends to follow the anisotropy of the electronic cloud associated with the $2p_z$ orbital. It can be written as

$$V_{:N-Ar} = E_0 \exp\left[-\left(\frac{x}{x_0}\right)^2 - \left(\frac{y}{y_0}\right)^2 - \left(\frac{z}{z_0}\right)\right] \tag{8}$$

where x, y, and z are the components, expressed in the molecular frame, of the vector between Ar and N.

Later in this paper, we will discuss more fully the nature of this empirical term. All the potential parameters used in the construction of the potential energy surfaces (PES) for the two electronic states are summarized in Table 1.

TABLE 1: Potential Parameters Used To Generate the PES Describing Interaction between Ar and Aniline in the Singlet S_0 and S_1 States

	S_0	S_1
ϵ_{C-Ar} (cm^{-1})	40.00	46.00
ϵ_{H-Ar} (cm^{-1})	33.00	37.50
ϵ_{N-Ar} (cm^{-1})	55.00	46.00
σ_{C-Ar} (Å)	3.42	3.37
σ_{H-Ar} (Å)	3.21	3.20
σ_{N-Ar} (Å)	3.28	3.28
E_0 (cm^{-1})		570.00
x_0 (Å)		0.85
y_0 (Å)		1.47
z_0 (Å)		4.00

3.B. Characterization of the Isomerization Dynamics. As was found in similar aromatic/rare gas clusters, it turned out to be useful to discuss the structure of aniline$-Ar_n$ clusters in terms of the distance of the rare gas atoms from the plane of the phenyl ring. The rather general notation (n,m|p|q,r) denotes a cluster with m and q argon atoms in a first solvation layer on either side of the ring, n and r atoms in a second solvation layer, and p atoms in the plane of the ring, acting as a bridge between the two sides. If no bridging atoms are present, the notation above can be simplified to (n,m|q,r). If only the first solvation layer is occupied, it reduces to (m|q).

To characterize dynamics in such a vdW system, we have calculated different parameters which we describe now. The kinetic temperature is defined by

$$T = \frac{2\langle KE\rangle_t}{3nk_b} \tag{9}$$

for the (aniline-rigid-body + n argon atoms) system; here $\langle KE\rangle_t$ is the time averaged kinetic energy of the cluster and k_b is the Boltzmann constant.

Root-mean-square values of bond length fluctuations have traditionally[2,33,41−43] been used to characterize the fluxionality of a cluster or nonrigid molecule; we employ two such quantities

$$\delta_{Ar-Ar} = \frac{2}{n(n-1)} \sum_{i=1}^{n}\sum_{j>i} \frac{(\langle r_{ij}^2\rangle - \langle r_{ij}\rangle^2)^{1/2}}{\langle r_{ij}\rangle} \tag{10}$$

where r_{ij} is the internuclear distance between argon atoms i and j and $\langle\ \rangle$ denotes a time average and

$$\delta_{An-Ar} = \frac{1}{n} \sum_{i=1}^{n} \frac{(\langle r_i^2\rangle - \langle r_i\rangle^2)^{1/2}}{\langle r_i\rangle} \tag{11}$$

In this latter equation, r_i is the distance between the ith argon atom and the center of mass of the aniline molecule. The two δ parameters generally increase smoothly with the internal energy of the system until some critical transition point is

reached; according to the so-called Lindeman criterion,[44] a system will usually melt at the very temperature at which δ jumps abruptly through the value 0.1. For the present investigation, the two δ parameters measure intrinsically different quantities; δ_{An-Ar} measures the mobility of the argon atoms relative to the aniline substrate, while δ_{Ar-Ar} measures the relative mobility of the solvent atoms alone.

3.C. Spectral Simulations. In this section, we describe the spectral density method which has first been developed to reproduce the spectral broadening appearing in macroscopic systems.[45−47] In many cases, molecular systems can be described by a two-level model. For the vdW aniline−Ar$_n$ clusters, the hamiltonian (in the Born−Oppenheimer approximation) can be written as

$$H = |0\rangle\left[H_0(\mathbf{Q}) - \frac{i}{2}\gamma_0\right]\langle 0| + |1\rangle\left[H_1(\mathbf{Q}) - \frac{i}{2}\gamma_1\right]\langle 1| \quad (12)$$

with

$$H_0(\mathbf{Q}) = T_0(\mathbf{Q}) + V_0(\mathbf{Q})$$

and

$$H_1(\mathbf{Q}) = T_1(\mathbf{Q}) + V_1(\mathbf{Q})$$

$T_0(\mathbf{Q})$ and $T_1(\mathbf{Q})$ are, respectively, the kinetic energy operators in the S_0 and the S_1 states. $V_0(\mathbf{Q})$ and $V_1(\mathbf{Q})$ represent the potential energy operators in the same two electronic states.

$\mathbf{Q}$ represents the set of internal coordinates of the cluster which describe relative motions of the nuclei. The eigenvectors $|0\rangle$ and $|1\rangle$ correspond to the electronic states S_0 and S_1, respectively, while γ_0 and γ_1 are the inverse radiative lifetimes of the two states. In the case of aniline, the radiative lifetime in S_1 is about 10 ns, which corresponds to a very weak broadening as compared to the broadening which will be considered here due to vdW vibrations. Therefore we have taken $\gamma_0 = \gamma_1 = 0$.

The two electronic states will be coupled by the electric dipole moment operator $W(t)$ defined by

$$W(t) = D(\mathbf{Q})\, E(t)[|1\rangle\langle 0| + |0\rangle\langle 1|] \quad (13)$$

where $E(t)$ is the external electric field applied to the molecular system and $D(\mathbf{Q})$ is the dipole operator of the system depending on the internal coordinates $\mathbf{Q}$.

In the spectral density approximation, the normalized spectral shape of the electronic transition can be written as the Fourier transform of the dipole quantum autocorrelation function, $I(t)$, defined by[45,48,49]

$$I(t) = \langle \mu_{01}(0)|\mu_{10}(t)\rangle \quad (14)$$

which can be written as

$$I(\omega) = \frac{1}{\pi}\,\mathrm{Re}\int_0^\infty \mathrm{d}t\, \exp\left(-\mathrm{i}(\omega - \omega_{01})t - \frac{1}{2}(\gamma_0 + \gamma_1)t\right) I(t) \quad (15)$$

Here, ω_{01} is the frequency of the electronic transition for the bare aniline molecule.

In eq 14, the notation $\langle A\rangle$ corresponds to the quantum correlation function of the A operator which is defined by $\langle A\rangle = \mathrm{Tr}(A\rho_0)$ where ρ_0 corresponds to the canonical density matrix in the ground electronic state S_0 at thermodynamical equilibrium.

The $\mu_{10}(t)$ operator represents the electronic transition dipole moment which can be written in the Heisenberg formalism

$$\mu_{10}(t) = \exp(iH_1(t))\mu_{10}(0)\exp(-iH_0(t)) \quad (16)$$

with

$$\mu_{10}(0) = \langle 1|D(\mathbf{Q}(t{=}0))|0\rangle$$

In this paper, we are interested only in the simulation of spectra appearing in the vicinity of the origin of the electronic transition $S_1 \leftarrow S_0$. We therefore neglect the dependence of D on the intramolecular and vdW coordinates. In the rest of this paper we take $\mu_{01}(0) = 1$.

Combining eqs 14−16, $I(t)$ can be written as

$$\begin{aligned} I(t) &= \langle \mu_{01}(0)|\mu_{10}(t)\rangle \\ &= \mathrm{Tr}[\exp(iH_1t)\exp(-iH_0t)\,\rho_0] \\ &= \langle \exp(iH_1t)\exp(-iH_0t)\rangle \end{aligned} \quad (17)$$

S. Mukamel[50] showed that this last equation could be rewritten as

$$I(t) = \langle \exp[i\textstyle\int_0^t \mathrm{d}t_1\, U(t_1)]\rangle \exp[i\langle V_1 - V_0\rangle t] \quad (18)$$

with $\langle V_1 - V_0\rangle$ equal to the time-averaged value of the energy difference between the two adiabatic potential surfaces $V_1(t)$ and $V_0(t)$ and

$$U(t) = (V_1(t) - V_0(t)) - \langle V_1 - V_0\rangle \quad (19)$$

The spectral characteristics can be deduced from the temporal function $U(t)$ which gives the fluctuations (around the mean value) of the difference between the two adiabatic potential surfaces.

From eqs 18 and 19 and by only considering the first three terms of the expansion of $[i\int_0^\tau \mathrm{d}t_1\, U(t_1)]$ in eq 18, $I(\omega)$ can be written as

$$I(\omega) = \frac{1}{\pi}\,\mathrm{Re}\int_0^\infty \mathrm{d}t\, \exp(-\mathrm{i}\Lambda t - g(t)) \quad (20)$$

with

$$\Lambda = \omega - \omega_{01} - \langle V_1 - V_0\rangle \quad (21)$$

and

$$g(t) = \int_0^t \mathrm{d}t_1 \int_0^{t_1} \mathrm{d}t_2\, J(t_2) \quad (22)$$

In eq 22, $J(t)$ is the autocorrelation function of $U(t)$; $g(t)$ can finally be written as

$$g(t) = -\int_{+\infty}^{-\infty} \mathrm{d}\omega\, \frac{J(\omega)}{\omega^2}[\exp(i\omega t) - \mathrm{i}\omega\mathrm{t} - 1] \quad (23)$$

with

$$J(\omega) = \frac{1}{2\pi}\int_{+\infty}^{-\infty} \mathrm{d}t\, \exp(-i\omega t)\, J(t) \quad (24)$$

In this way the spectral line shape can be deduced from $g(t)$, which can be expressed as a function of the power spectrum $J(\omega)$. S. Mukamel has shown that $g(t)$ can be evaluated from classical variables[51] by

$$g(t) = -\sum_j 2\left|\frac{A_j}{\omega_j}\right|^2 [k_j(\exp(i\omega_j t) - i\omega_j t - 1) + (1 - k_j)(\exp(-i\omega_j t) + i\omega_j t - 1)] \quad (25)$$

where the A_j are the Fourier components of $U(t)$ and k_j is given by

$$k_j = \frac{1}{1 + \exp\left(-\frac{\omega_j}{k_b T}\right)} \tag{26}$$

Equations 25 and 26 have been obtained by considering a semiclassical correction to evaluate the quantum operator, $J(\omega)$. Indeed the *fluctuation−dissipation* theorem[52,53] allows one to estimate the quantum power spectrum from the classical $J_c(\omega)$ power spectrum by

$$J(\omega) = \left[1 + \tanh\left(\frac{\omega}{2k_b T}\right)\right] J_c(\omega) \tag{27}$$

We use classical MD trajectories to obtain the semiclassical vibronic spectrum of the clusters of interest. To generate independent initial conditions, we have used the following scheme:

(i) A preliminary canonical dynamics is generated at a temperature T with the algorithm proposed by Nosé.[54] During this constant temperature trajectory, the energy of the system is tested; if it is within a band of width 1.5 cm^{-1} centered at the corresponding mean value of the energy at this temperature, the instantaneous values of the dynamical variables are accepted as initial conditions for a microcanonical trajectory. This procedure is repeated until the desired ensemble of independent initial conditions is obtained.

(ii) These initial conditions are then used to propagate microcanonical trajectories of duration equal to 107.46 ps. Each trajectory at constant energy generates a subspectrum in accordance with the theoretical scheme described above. This scheme is realized numerically as follows. The function $[V_1(t) - V_0(t)]$ is evaluated at 1024 points evenly spaced in time (each 105.04 fs). The Fourier components A_j (eq 25) of the function $U(t)$ (eq 19) are obtained by use of the fast Fourier transform (FFT) algorithm. To avoid edge effects associated with the FFT, we multiply $U(t)$ by a Blackman−Harris filter function.[55]

Now $g(t)$ is evaluated from eq 25. A subspectrum is obtained by evaluating the Fourier transform of the function $e^{-g(t)}$ (eq 20). The final spectrum is obtained by averaging a given set of independent subspectra.

To calculate the spectral shift, we have introduced a correction term to take into account the nonequivalence of the sites located on either side of the aromatic plane due to the nonplanarity of the assumed rigid geometry of aniline in its ground electronic state. This correction term takes into account the quantum nature of the inversion motion of hydrogen atoms in the $-NH_2$ group (neglected in the classical simulation); indeed, solving the Schrödinger equation for this degree of freedom in a realistic potential shows that this inversion motion is perturbed but not blocked.

This term naturally depends on the difference (ΔE) between the binding energies of the two structures obtained by symmetry with respect to the aromatic plane, $\Delta E = D_e(Q_0) - D_e(-Q_0)$, where Q_0 is the equilibrium value of the inversion coordinate. More details about the evaluation of this term can be found in a previous paper (see Appendix A in ref 23). It relies on the linearization of the vdW potential dependence upon the inversion coordinate. However, unlike the case of a single argon atom in which the asymmetry is small and consequently the correction term in the vdW spectral shift is just $\Delta E/2$, when the number of argon atoms is larger the asymmetry is no more proportional to ΔE. The results of this treatment are summarized in Figure 2.

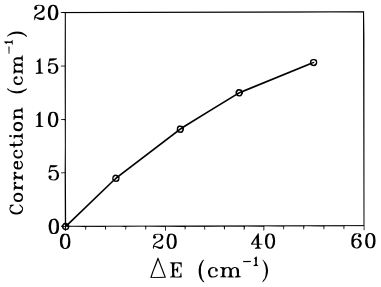

Figure 2. Plot of the correction term to the electronic shift versus asymmetry in binding energy. This term results from the nonequivalence of the two minimum energy structures (nearly symmetrical with respect to the aromatic plane) due to the nonplanarity of the rigid aniline molecule (see text). ΔE is the difference between the binding energies of the two structures.

During the microcanonical trajectories, we also calculated the dispersion (Δ) of the $U(t)$ function

$$\Delta = \sqrt{\langle U_2 \rangle - \langle U \rangle^2} \tag{28}$$

The parameter Δ summarizes some dynamical information about the system, and in particular, the influence of nuclear dynamics on the spectroscopic properties can be understood.

It can be shown that, in the case of a Gaussian distribution of the spectral density, the full-width-at-half maximum (fwhm) of this Gaussian is related to Δ by

$$\text{fwhm} = 2.35\Delta \tag{29}$$

Thus, the parameter Δ is exactly equal to the second moment of the spectrum.[45,56] Some recent studies[17,57] have used this quantity as well as the first moment or spectral shift to analyze the evolution of the spectral shape of similar vdW systems.

In their numerical study of inhomogeneous benzene−Ar_n clusters, Fried and Mukamel[58] have discussed their results by characterizing three different dynamical regimes.

(i) Case I, *oscillatory regime*: the autocorrelation function can be written as $J(t) = J(0)\cos(\omega t)$. In this case, the spectrum will be composed of a succession of narrow vibrational bands.

(ii) Case II, *damped oscillatory regime*: the autocorrelation function can be written as $J(t) = J(0)\cos(\omega t)\exp(-t/t_c)$, where t_c is the characteristic damping time. This time can be associated with the inverse of the mean value of the frequencies of the fluctuations. This damping will naturally induce a broadening of the bands. The larger the parameter Δ (eq 28), the stronger this effect will be.

(iii) Case III, *static regime*: this last case corresponds to the situation where the perturbing environment (Ar atoms) can be considered as static. In this particular case, the semiclassical theory predicts a spectral profile of Gaussian shape with a fwhm given by relation 29.

4. Results and Discussion

4.A. Aniline−Ar and Aniline−Ar_2. *4.A.1. Experimental and Theoretical Spectra.* We discuss first here the electronic spectrum of the aniline−Ar complex, because for this simplest cluster it is possible to compare the results of semiclassical simulation with the results (electronic shift, frequencies, and intensities of the vdW excited bands) of both experiment and exact fully-quantum 3D calculation.[23]

The experimental spectra of the vdW clusters with one to four argon atoms are reproduced in Figure 3. The very same spectra have been already shown in ref 61 which was devoted to the vdW frequencies assignments. The frequencies are given relative to the position of the origin band of the aniline

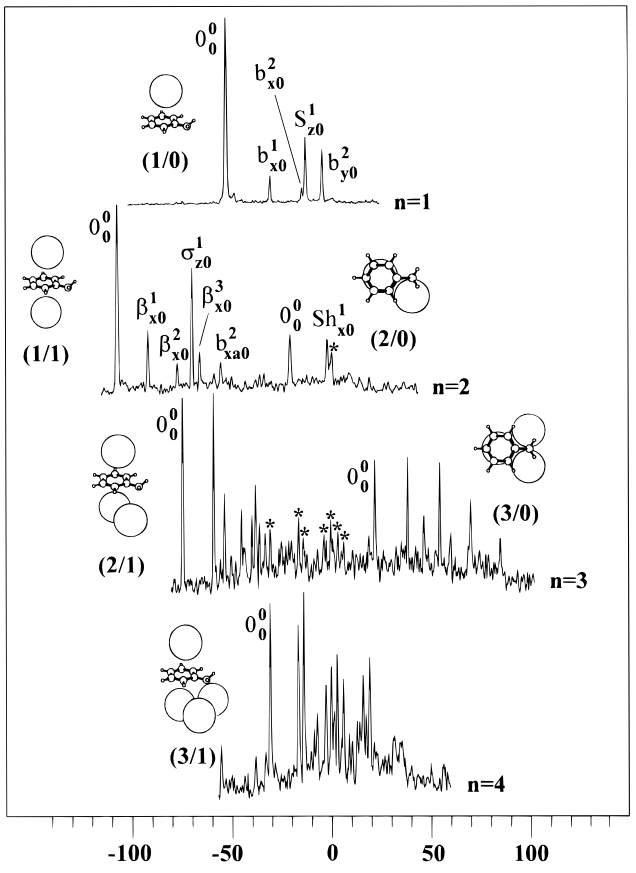

Figure 3. Experimental R2P2CI spectra of the aniline−Ar$_n$ clusters ($n = 1-4$) taken with 2% Ar/He gas mixture expanded from stagnation pressure $P_0 = 5$ bar. For $n = 1$ and 2 spectra, the assignments of all observed vdW vibrational bands are indicated. For $n = 3$ and 4, only the origins of each structural isomer are labeled. The stars show in the $n = 2$ spectrum a band resulting from superimposition with the origin of the monomer and show in the $n = 3$ spectrum bands due to residual fragmentation from the aniline−Ar$_4$ cluster. The frequency scale refers to the origin of the monomer 0_0^0 band.

TABLE 2: vdW Frequencies (in cm^{-1}) for the Aniline−Ar Complex

			theoretical frequencies			
	experimental frequencies		3D-quantum ref 23		semiclassical (this work)	
vdW mode	S_0	S_1	S_0	S_1	S_0	S_1
b_x $\upsilon = 1$	18.6,[a] 19.6[b]	22.1	12.6	18.1	14.3	18.6
b_x $\upsilon = 2$		37.7	25.1	33.8	28.6	
S_z $\upsilon = 1$		39.6	46.6	42.3	44.1	46.5
b_y $\upsilon = 1$	35.7[b]		22.0	25.6		
b_y $\upsilon = 2$		47.8	38.1	53.6		

[a] From hot band b_{x1}^1. [b] From Raman spectra ref 60.

monomer, contrary to what was done in ref 61, where the frequency scales had been shifted to superimpose the origins of the various (n/0) and (n/1) isomers. Additionaly, it should be noted that spectra of the $n = 1-5$ species have already been recorded by Bieske et al.[59] and by our group[9] for the $n = 1-6$ species. The most noticeable difference appearing in Figure 3 is the great amelioration in the spectral resolution mainly due to the better cooling of the molecular species in the supersonic jet.

A relatively large number of narrow bands are visible in these spectra, which immediately indicates that vdW vibrations are significantly active in the electronic transitions of these species.

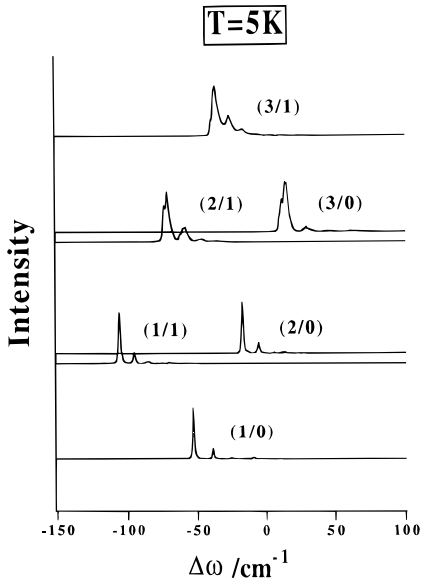

Figure 4. Simulated spectra for various isomers of the aniline−Ar$_n$ clusters ($n = 1-4$) at $T = 5$ K. The frequency scale is as in Figure 3. The residual structure, hardly visible in the $n = 3$ spectra, is expected to disappear by increasing the statistics of subspectra.

TABLE 3: Comparison between the Experimental and Calculated Electronic Shifts (in cm^{-1}) for the Various Structural Isomers of Aniline−Ar$_n$ ($n = 1-3$) Clusters

isomer	experimental	calculated
(1|0)	−53.2	−53.3
(1|1)	−107.4	−106.1
(2|0)	−20.8	−16.9
(3|0)	+21.9	+14.8
(2|1)	−74.4	−71.3

The assignments of the vibrations of the clusters with one and two argon atoms, indicated in Figure 3 (top two panels), have been discussed in our previous paper.[9] In the present spectrum of $n = 1$, we have been able to discriminate perfectly the two vdW bands b_{x0}^2 and S_{z0}^1 and then to confirm our first assignment.[9] As a matter of fact, this assignment has been recently questioned by Maxton et al.[60] in a critical comparison with their Raman spectra. Such spectra are, by nature, mostly sensitive to the bending fundamentals in the ground electronic state S_0, which were found at 19.6 cm^{-1} for b_{x1} and 35.7 cm^{-1} for b_{y1} in the (1/0) complex. To the blue of the origin band in the spectrum of $n = 1$, a small band is assigned to the b_{x1}^1 (see ref 61) from which we derive $b_{x1} = 18.6$ cm^{-1}, in fairly good agreement with the Raman value. Comparison of the frequencies for the $\upsilon = 1$ b_y mode in both electronic states ($b_{x1} = 35.7$ cm^{-1}, $b_y^2 = 49$ cm^{-1}) suggests that the PES is strongly anharmonic in the energy range of about 50 cm^{-1} above the ground vdW state. This was indeed noted in our 3D quantum calculation.[23] A full list of frequencies is given in Table 2.

In Figure 4 are reported the theoretical electronic spectra of the aniline−Ar$_n$ clusters ($n = 1-4$) calculated at $T = 5$ K by the semiclassical simulation technique explained in Section 3.C. As apparent from Table 3, the electronic spectral shift of the $S_1 \leftarrow S_0$ transition in the aniline−Ar complex (−53.3 cm^{-1}) is in excellent agreement with the experimental value (−53.2 cm^{-1}) and also with the theoretical value (−53.2 cm^{-1}) derived from the 3D quantum calculation made using the same potential energy surfaces.[23] This indeed is not surprising since the excited state PES was adjusted[23] in that perspective. The fwhm of the bands of this cluster is smaller than 1.5 cm^{-1} and reproduces the experimental spectral width. As a matter of fact, the experimental bandwidth is essentially in that case the *contour*

resulting from a distribution of many rotational lines affected by convolution with the instrumental bandwith. On the other hand, the simulated width is indeed related (also in that case) to the size of the energy band (1.5 cm^{-1}) which was used in the preliminary Nosé trajectory aimed at generating the initial conditions for the microcanonical trajectories. This may explain why an apparent change of the width with cluster size is seen in the simulated spectra: since the relative energy fluctuation in a microcanonical system decreases when the number of particles increases, the fixed 1.5 cm^{-1} bandwidth tends to accept initial conditions which depart gradually more from equilibrium.

One interesting point in this semiclassical simulation is the observation of several different vdW peaks (corresponding to the vibrations of the Ar atom with respect to the substrate). In their theoretical study of benzene−Ar_n, Fried and Mukamel[58] observed only one vdW peak (at around 40 cm^{-1}) assigned to the stretching mode, which was in good agreement with experiment. In the present case, the simulation shows a much richer spectrum due to the lower symmetry of the aniline−Ar complex.

The values of the vdW frequencies derived from this simulation are included in Table 2 for comparison with other experimental and theoretical values. Although the S_z stretching frequency is well reproduced, the bending frequency along the *x*-direction is severely underestimated by the semiclassical calculation. At first sight this result seems surprising because the same PESs were used in the quantum treatment which gave better agreement with experiment.[23] To understand this difference between the quantum calculation and the semiclassical simulation, another spectrum (with the same initial conditions) has been simulated by artificially propagating the classical trajectories in the excited electronic state S_1, in contrast with the previous case where the propagation was normally done in the ground electronic state S_0 to reflect absorption spectra. Two clear differences appear:

(i) The spectrum is shifted to the red when the temporal propagation is run in the S_1 state. This difference (=10.6 cm^{-1}) can be explained by the fact that we do not test the same region of the PES because the two surfaces are clearly not parallel, being particularly strongly displaced along the *x*-axis.

(ii) The calculated vdW frequencies are noticeably larger when the propagation is realized in the S_1 state. The b^1_{x0} transition, associated to the one-quantum excitation of the bending mode along the *x*-axis (parallel to the C−N bond), increases from 14.3 to 18.6 cm^{-1}. It is interesting to note that this new value is close to the result obtained from the quantum calculation (18.1 cm^{-1}). On the other hand, the stretching frequency increases from 44.1 to 46.5 cm^{-1}. The quantum calculation of the eigenstates in the S_1 state revealed a smaller value (42.3 cm^{-1}). This result confirms our first interpretation, already discussed in ref 23, that a strong anharmonic coupling between S^1_z and b^2_y states is present, inducing a decrease of the stretching frequency in the quantum treatment.

In the semiclassical simulations, this last band is not observed. Indeed the two PESs are not displaced along the *y*-axis. As a consequence, activation of this motion only induces a very weak variation of the difference potential function $U(t)$. For this particular mode, we are in a situation similar to that of benzene−Ar where the PESs are almost parallel.

As it was the case in the quantum calculation, the simulated intensities for the two bands involving the *x*-bending modes are in good agreement with the experimental values. On the other hand, the intensity of the S^1_{z0} band is largely underestimated. The fact that both semiclassical and quantum methods give the same erroneous result for this intensity strengthens our suspicion that the PESs themselves are responsible for that defect. It is also interesting to note that intensities are approximately unchanged when the vdW dynamics is run in S_1. It is most likely that the atom−atom potentials used in the simulation fail to properly account for the changes in the Ar−aniline distance induced by the $\pi \rightarrow \pi^*$ electronic excitation.

Even though this semiclassical method has been developed to simulate spectra in large systems, it is noteworthy that results obtained with only one Ar atom are in reasonable agreement with those derived by the fully-quantum method. However, it is clear that some difficulties, inherent in the method, are present. Obtaining a good agreement for both the spectral electronic shifts and the intermolecular frequencies seems to be very difficult when the two PESs differ substantially (i.e., are displaced along at least one coordinate). For the small systems where vibrational information is available, this semiclassical method is limited by the fact that the spectral information is obtained from the $U(t)$ function calculated during a classical trajectory propagated in the ground electronic state S_0, thus reflecting the Fourier frequencies of this ground PES. *This drawback will not be serious in large systems where* ***detailed*** *vibrational information is no longer available (see paper 2).*

We turn now to a discussion of the spectra of aniline-Ar_2 clusters, which also exhibit a series of well-resolved vdW excited bands. Indeed the experimental spectrum (see Figure 3) recorded on the mass channel 173 amu extends from −106 to about 0 cm^{-1}. This very large frequency range is due to the existence of two different structural isomers, already identified as (1|1) and (2|0).[9,61] The calculated minimum energy structures of these two isomers are also shown in Figure 3 next to the corresponding R2P2CI spectra. A strong specificity of the electronic shift is observed depending on the localization of the Ar atom relative to the aromatic substrate. This strong electronic specificity has also been confirmed by recent measurements of the ionization threshold for these two isomers.[62]

The spectra simulated at T = 5 K for these two isomers can be seen in Figure 4. The experimental and theoretical values of the electronic shifts for the 0^0_0 transition are summarized in Table 3. Good agreement between experiment and theory is found. In particular, the two PESs allow to account for the strong specificity of the two main adsorption sites. The $V_{:N-Ar}$ term (eq 8) in the S_1 state PES, described in section 3.A, plays an important role in the quality of the agreement with the experimental values, in particular when one Ar atom is in strong interaction with the nitrogen atom (isomer (2|0)). This *special* parametrization of the interaction between Ar and N seems to confirm the specific role of the nitrogen atom lone pair in the solvation process of the aniline molecule by Ar atoms.

The simulated spectra (Figure 4) reveal the presence of intense vibrational bands. The most accurate experimental data on the vdW frequencies have been obtained for the (1|1) isomer. Different authors [3,9,63] have clearly observed three intense vdW bands assigned to the symmetrical bending mode along the x-axis (β^1_{x0}, β^2_{x0}) and to the symmetrical stretching mode (σ^1_{z0}). Recently, Douin and Bréchignac[61] have observed two new vibrational bands which have been assigned to the third overtone of the symmetrical mode along the x-axis (β^3_{x0}) and to the second overtone of the antisymmetrical bending mode along the same direction (b^2_{xa0}). It is interesting to check whether the semiclassical simulation reproduces all these experimental values. The comparison is summarized in Table 4. As in the case of aniline−Ar, the frequency associated with the stretching mode is in excellent agreement with the experimental value while, in the case of the symmetrical bending mode along the

TABLE 4: Experimental and Theoretical vdW Frequencies (in cm^{-1}) for the Aniline−Ar$_2$ (1|1) and (2|0) Clusters

vdW modes	experimental frequencies	theoretical frequencies
	(1|1) Isomer	
β^1_{x0}	15.1	10.5
β^2_{x0}	29.9	21.1
σ^1_{z0}	37.2	36.0
β^3_{x0}	45.3	
b^2_{xa0}	54.8	
	(2|0) Isomer	
sh^1_{x0}	18.5	11.8
sh^1_{y0}		30.5
σ^1_{z0}		49.0

x-axis, the calculation tends to underestimate this frequency. Note, however, that the ratio of calculated to experimental frequencies is about the same for aniline−Ar$_2$ as for aniline−Ar (that is, $[\beta^1_{x0}/b^1_{x0}]^{(exptl)} \cong [\beta^1_{x0}/b^1_{x0}]^{(calcd)}$). The calculated intensities for the *x*-bending mode are in good agreement with the experimental ones. On the other hand, the intensity of the vdW band associated with the stretching mode (σ_z) is again seriously underestimated as discussed for the aniline−Ar complex.

In the case of the (2|0) isomer, the global pattern of the simulated spectrum is very similar to the (1|1) spectrum. Three vdW bands can be observed, whose frequencies are $\nu_1 = 11.8$, $\nu_2 = 30.5$, and $\nu_3 = 49.0$ cm^{-1}. Only the first one is intense in the calculated spectrum. If we compare these frequencies with the calculated frequencies for the (1|1) isomer, the first frequency ν_1 can be assigned to a mode associated to the overall motion of the Ar$_2$ dimer along the *x*-axis (shearing mode). This x-shearing frequency calculated in the (2|0) isomer (11.8 cm^{-1}) is slightly larger than the symmetrical *x*-bending mode frequency in the (1|1) isomer (10.5 cm^{-1}). This result is confirmed by the experimental findings: the frequencies associated to these two motions are respectively equal to 18.5 cm^{-1} in the (2|0) isomer and to 15.1 cm^{-1} in the (1|1) one.

Another interesting characteristic of the calculated spectrum for the (2|0) isomer is the appearance of a new frequency $\nu_2 =$ 30.5 cm^{-1} which seems too low to be considered as a stretching mode. In fact this frequency ν_2 can be associated with a motion of the Ar dimer along the *y*-axis or perhaps a rotation of this dimer involving mainly the motion of the Ar atom near the $-NH_2$ functional group. In a recent paper, Douin and Bréchignac[61] developed a simplified mechanical model to analyze vdW modes in aniline−Ar$_n$ clusters whose size ranges from $n = 1$ to 4. For the (2|0) isomer, the frequency associated with the bending motion along the *y*-axis (shearing motion) was predicted to be equal to 25.8 cm^{-1}, which is in reasonable agreement with the presently calculated ν_2 frequency. In order to check the validity of this prediction, a velocity autocorrelation function analysis has been done. The power spectra have been calculated for the components of the Ar$_2$ dimer center of mass velocity in the aniline frame along the three directions *x*, *y*, *z*, using a set of random initial conditions. The components along *x* and *y* both exhibited power around 10 and 30 cm^{-1} with alternate relative intensities (respectively larger at 10 cm^{-1} for the *x*-axis and 30 cm^{-1} for the *y*-axis). The component along *z* exhibited most of the power at 47 cm^{-1}. Although because of the lack of symmetry, the shearing frequencies can hardly be considered as pure, this analysis confirms the assignment of ν_1 and ν_2, while ν_3 is assigned to the stretching mode along the *z*-axis. It is important to note that the ν_2 and ν_3 frequencies are not clearly apparent in the experimental spectrum.

TABLE 5: Evolution of the Electronic Shift (in cm^{-1}) versus Temperature in the Case of the (1|1) and (2|0) Isomers of Aniline−Ar$_2$

T (K)	(1|1) isomer	(2|0) isomer
5	−106.1	−17.4
10	−101.1	−13.7
15	−96.2	−11.2
20	−91.2	−8.1

4.A.2. Temperature Effect in the (1|1) and (2|0) Isomers. The semiclassical spectral method was primarily used in this work as a guiding tool for the interpretation of the experimental findings. It is indeed well suited for analyzing the influence of the vibrational temperature on the spectral line shape. More specifically one of the main motivations for this work was to check the sensitivity of the spectral properties to well-defined dynamical phenomena which can appear in free clusters like phase transitions or more commonly isomerization transitions. The feedback between experiment and theory is of course of importance, the theoretical studies providing, in turn, a route to estimating the typical internal temperature of the clusters in various spectroscopic experiments.

The following discussion is mainly focused on the theoretical results derived from spectral simulations for the two structural isomers of the aniline−Ar$_2$ clusters, namely the (1|1) and (2|0) isomers.

Two main reasons motivate this choice:

(1) The small size of these clusters is a favorable factor for the feasibility of experimental observation of phenomena which are revealed by the simulations.

(2) The simulation of the internal dynamics in the (1|1) and (2|0) isomeric clusters has been analyzed in detail in a separate paper.[27]

We consider first the electronic shift in the simulated spectra of the (2|0) isomer: it can be seen from Table 5 that the red shift of the 0^0_0 transition displays a decrease when the kinetic temperature increases. A similar tendency is observed for the (1|1) isomer. Fried and Mukamel[58] and Heidenreich and Jortner[64] also observed the same behavior in their simulations, respectively, for the benzene−Ar$_n$ and tetracene−Ar$_n$ clusters. Although this is a classical simulation, this behavior may be understood by analogy with the appearance of hot bands associated to the population of vdW modes. The increase of temperature in a quantum system implies an increase of the population of low-lying vibrational levels in S_0. Here naturally the hot bands are blue shifted because the vdW frequencies are larger in S_1 than in S_0. This phenomenon should be easier to observe experimentally in the larger clusters because the number of vibrational degrees of freedom (=3*n*) is larger and then the density of vibrational states will quickly become very large. Consequently the first vibrational states will be effectively populated at relatively lower temperatures. Nonetheless such a blue degrading of the band shape has often been observed in the small aniline−Ar$_{1,2}$ clusters. From the spectrum of the (1|0) isomer in Figure 3, assignment of the b^1_{x1} band allows estimation of a vibrational temperature of ∼8 K. In other experimental conditions the merging of several hot bands has been observed:[9,59] for instance the analysis of the $n = 1$ spectrum obtained simultaneously (in the same frequency scan) with the spectra shown in Figure 10 below leads to a vibrational temperature of ∼15 K. This increase of vibrational temperature from conditions of the spectra in Figure 3 to conditions of the spectra in Figure 10 is consistent with a similar increase of the rotational temperature, as revealed by the change in the width of the main band (by about a factor of 2).

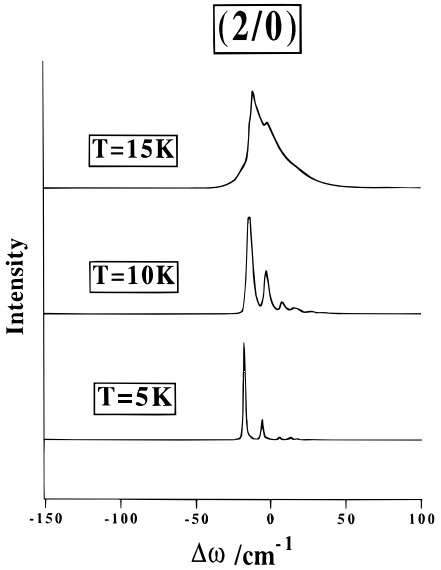

Figure 5. Simulated spectra for the (2|0) isomer at three different temperatures: $T = 5$, 10, and 15 K. The frequency scale is as in Figure 3.

We come now to a discussion of the specific effects observed in the line shapes of the simulated spectra of the (2|0) isomer as we raise the kinetic temperature. These theoretical spectra are drawn in Figure 5 for three different temperatures ($T = 5$, 10, and 15 K). Each spectrum was obtained from an average over 15 independent subspectra. A strong spectral broadening appears around $T = 15$ K. At this temperature the simulated electronic spectrum becomes structureless, although some intense vdW bands are visible at lower temperatures. The observed broadening in the line shapes can be due to two factors very different in nature.

The *homogeneous* broadening is generally considered as the consequence of fluctuations of the frequency associated with the transition. These fluctuations can be viewed as the consequence of nonperiodic motions of the molecular system around its equilibrium configuration. An *inhomogeneous* spectral broadening can appear as the result of the presence of many isomers with slightly different spectral shifts resulting from the fact that the interaction with the chromophore depends on the positions of the argon atoms. If many isomers are communicating (isomerization phenomena), the concept of homogeneous versus inhomogeneous broadening will strongly depend on the ratio of the characteristic isomerization rate to the characteristic frequency of vibration around the local minimum in the PES. Indeed if the isomerization rate is small as compared with the inverse of the characteristic vibrational period, we deal with inhomogeneous broadening since the system can be considered as an assembly of many isomers in weak communication which vibrate around their equilibrium structures. On the other hand, when the interchange frequency is fast, large amplitude motions take place and the system explores a large fraction of the phase space. It is noteworthy that these two limits, homogeneous and inhomogeneous, are often used in the spectroscopic description of the solid phase, and in particular for molecules trapped in matrices.[65,66]

In order to explain the net change in the spectral line shape, we have analyzed the fwhm for each subspectrum. Indeed if we observe that the spectral widths of individual subspectra remain small while the average spectrum (averaged on the subspectra) exhibits a large width, we can conclude that the global broadening is due to the presence of numerous isomers with different absorption frequencies. In the opposite case, the widths of the bands will be homogeneous. The results are the following: at low temperature, all the subspectra have essentially the same small fwhm. On going to a higher temperature regime (above 15 K), the distribution of the fwhm of the subspectra is spread out by itself. The system is then in a dynamical regime where subspectra of very different spectral widths are simultaneously present, in particular some widely broadened subspectra make a large homogeneous contribution to the total width. In order to understand this phenomenon, microcanonical trajectories have been run to see if it can be associated with a particular dynamical behavior. On the basis of direct examination of selected dynamical variables for the (2|0) isomer in MD simulations,[27] the interpretation of the observed broadening in the spectral simulations is indeed greatly facilitated. From the work published separately about the dynamics in aniline$-Ar_2$, we conclude that the net change in the (2|0) spectral line shape appears at $T = 15$ K, which is the temperature of the onset of a surface transition:[27] at this temperature, one argon atom begins to execute very large amplitude low-frequency motions while staying almost in a plane parallel to the aniline molecule.

Further analysis of MD trajectories reveals that, above this temperature, more complicated motions appear, involving a complete decoupling of the Ar_2 dimer from the substrate. In this high-energy range, the configuration of the cluster is not any more well defined. The system moves through a large portion of the phase space. In addition to these low-frequency periodic motions, nonperiodic motions also appear, evolving to a chaotic regime. Consequently, the spectrum is broadened as in the case II described above. In contrast to the benzene$-Ar_n$ system, studied by Fried and Mukamel,[58] the aniline/argon interaction displays a larger range of values when the argon atom explores different sites, leading to a larger value for Δ and a greater sensitivity to dynamical motions with respect to the substrate.

As a final remark, one may argue that this broadening might have been a major reason for the lack of observation of the (2|0) isomer until recently[9] where it was recognized that a very good cooling efficiency was necessary. Indeed the theoretical surface transition temperature (15 K) is perfectly consistent with the estimations of the vibrational temperature (8−15 K) derived from experimental spectra (see above).

4.B. Aniline$-Ar_3$. *4.B.1. Experimental and Theoretical Spectra for $n = 3$.* The $n = 3$ cluster accommodates two stable structural isomers, namely the (3|0) and (2|1) clusters. Again comparison of Figure 4 with Figure 3 shows that the simulated spectra reproduce the experimental electronic shifts very well (see also Table 3). Again, as noted for the (1|0) and (2|0) isomers, this agreement is sort of "built-in" in the PESs , confirming the assignment of the structures and the validity of the simulation method. The experimental electronic absorption spectrum of the (3|0) isomer (Figure 3) also clearly shows the presence of an extended vibrational progression whose frequency is equal to $\nu_1 = 16.5$ cm^{-1}. The spectral simulation almost perfectly reproduces this frequency ($\nu_1 = 17.0$ cm^{-1} (Figure 4)). As already said before, the semiclassical simulation is very sensitive to the atomic motions along the long *x*-axis. Consequently it seems reasonable to associate this frequency to the overall motion of the Ar_3 trimer in the *x*-direction, assigned as a "shearing" mode in ref 61. Indeed a velocity autocorrelation function analysis performed for that isomer using random initial conditions confirmed this assignment. The power spectrum associated to the *x*-component of the Ar_3 center of mass velocity in the aniline frame exhibited a clear peak near 17.0 cm^{-1}. It must be noted, however, that the spectral simulation does not reproduce the observed intensity distribution of the various members of the progression.

From the experimental spectrum (Figure 3) futher information can be extracted on this same isomer. It shows the presence of two other vdW frequencies at 25.0 and 38.1 cm^{-1}. The analysis of the simulated spectrum also reveals the presence of two other fundamental frequencies (28.0 and 44.0 cm^{-1}) with weaker intensities. These two new frequencies are in relatively good agreement with the experimental values, considering the systematic finding that the frequencies obtained in the simulation are rather characteristic of the electronic ground state. The (3|0) isomer is of C_s symmetry as is the aniline−Ar complex. Only the totally symmetric vibrational states (A′ type) can be optically excited. It seems reasonable to assign the frequency at 38.1 cm^{-1} (experimental) as the excitation of one quantum in the stretching mode. As the modes associated with the *y*-motions are of A″ symmetry (antisymmetric), only the excitation of an even number of quanta in these modes will be allowed. Consequently, the experimental frequency at 25.0 cm^{-1} may be understood as the excitation of two quanta in the *y*-bending mode. This mode can be associated with the concerted motion of the argon trimer along this axis.

In the case of the (2|1) isomer, the simulation mainly reveals the presence of one vibrational mode whose associated frequency is equal to 13.0 cm^{-1}. The experimental spectrum (Figure 3) reveals nine bands (including the origin band). The most intense vibrationally excited band appears at 14.9 cm^{-1} from the origin band. This frequency is in good agreement with the theoretical value of 13.0 cm^{-1}. It can be assigned to the fundamental excitation of the *x*-bending mode. It can be noted that the calculation predicts that the *x*-bending frequency is lower for the (2|1) isomer than for the (3|0) which is confirmed by the experimental spectra. All the others bands, appearing in the experimental spectrum of the (2|1) isomer, have been assigned by Douin and Bréchignac[61] on the basis of a simplified restricted harmonic model.

The understanding of the spectroscopic properties of the vdW aromatic−rare gas atoms clusters is naturally intimately linked with the vibrational behavior of these weakly bound species. As seen in section 4.A.2, concerning the temperature effect on the simulated spectra for the (1|1) and (2|0) isomers, a strong relationship between the isomerization processes and the simulated spectral characteristics has been observed. This motivates the discussion of the isomerization dynamics included in the present paper for various cluster sizes.

4.B.2. Isomerization Dynamics in the (2|1) and (3|0) Isomeric Clusters. As in many investigations of cluster dynamics, we shall study the evolution of the properties of the system as a function of increasing internal energy. We consider first the (2|1) isomer and then the (3|0) cluster. In the first case we expect a similarity with the case of the (2|0) cluster. In the second case we should think of the presence of an argon trimer. In both cases, we shall ultimately observe the isomerization (2|1) ↔ (3|0). The usual parameters *T*, δ_{Ar-Ar} and δ_{An-Ar} have been calculated at fixed total energies ranging from −1250 and −600 cm^{-1}.

We focus first on the case of the two-sided (2|1) isomer which is less stable than the one-sided (3|0).[9] The plot of δ_{An-Ar} versus *E* (Figure 6b) reveals a net increase of this parameter around $E = -1035$ cm^{-1} ($T = 20$ K). However at the same internal energy, no significant change is seen in the curve of δ_{Ar-Ar}. Inspection of the caloric curve (Figure 6c) reveals a slight change in the slope around this energy. If we now look at the evolution of the Cartesian coordinates of the three Ar atoms versus time, the increase of δ_{An-Ar} and the slight nonlinearity of the caloric curve as a function of the internal energy can be correlated with the appearance of a new type of motion in the molecular system: the Ar atom at the $-NH_2$ site (adsorption site near the $-NH_2$ group) begins to communicate with its equivalent site (symmetrically located with respect to the *xz*-plane) by exhibiting windscreen wiper motions, as was observed in the case of the (2|0) isomer.[27] The appearance of such a *surface transition* at a relatively low temperature reveals an important and general characteristics of aromatic−(rare gas) systems: the topology of the PES allows for some very large amplitude anharmonic motions in the plane parallel to the chromophore.

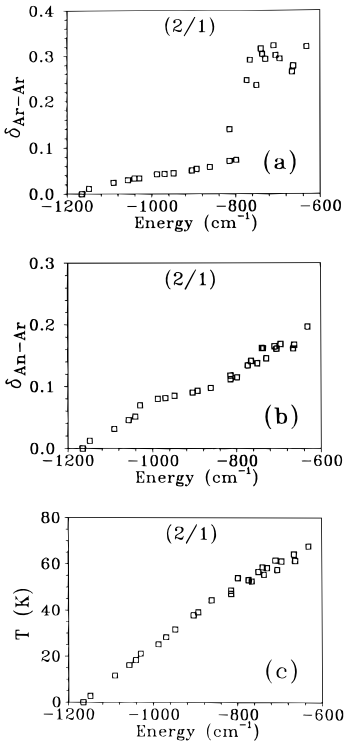

Figure 6. δ_{Ar-Ar} (a), δ_{An-Ar} (b), and *T* (K) (c) versus internal energy for the (2|1) isomer.

At $E = -814$ cm^{-1}, the δ_{Ar-Ar} parameter increases dramatically (Figure 6a) due to the onset of another type of isomerization process, the so-called *side-crossing* transition, which corresponds to the motion of Ar atoms from one side to the other side of the aromatic plane. The (2|1) and (3|0) isomers are then communicating. This 3-D type transition appears at $T = 48$ K.

We turn now to the analyzis of the dynamics in the more stable one-sided (3|0) isomer. It is reflected in the three curves of Figure 7 showing *T*, δ_{An-Ar} and δ_{Ar-Ar} as a function of total energy *E*. A surface transition also appears at around $E = -1120$ cm^{-1} ($T = 17$ K) revealed by a net increase of δ_{An-Ar} (Figure 7b). The linear behavior of δ_{Ar-Ar} around this value of *E* (Figure 7a) shows that the rigid Ar_3 trimer moves in a concerted fashion. To visualize the decoupling of the Ar_3 trimer with respect to the substrate, the positions of each of the three labeled Ar atoms in a plane parallel to the aniline molecular plane at equally separated time intervals have been plotted in Figure 8 during a 1.5 ns trajectory at $E = -1120$ cm^{-1}. On this graph, the curved arrows help to visualize the atomic motions which appear at the same time inducing an overall rotation by an angle of $2\pi/3$ of the Ar_3 trimer with respect to the substrate.

The δ_{Ar-Ar} curve displays a regular increase between −1100 and −800 cm^{-1}, with, however (in contrast to the (2|1) isomer), a change of slope around $E = -930$ cm^{-1} ($T = 38$ K). At this energy δ_{Ar-Ar} already satisfies the Lindemann criterion ($\delta >$

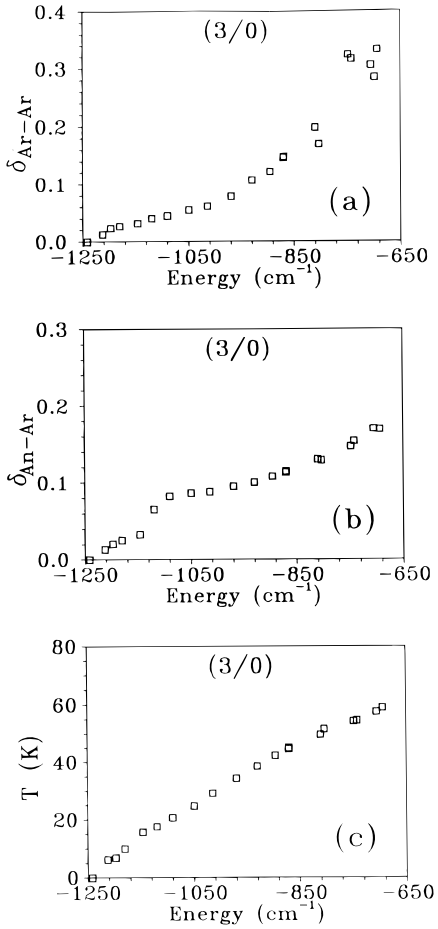

Figure 7. δ_{Ar-Ar} (a), δ_{An-Ar} (b), and T (K) (c) versus internal energy for the (3|0) isomer.

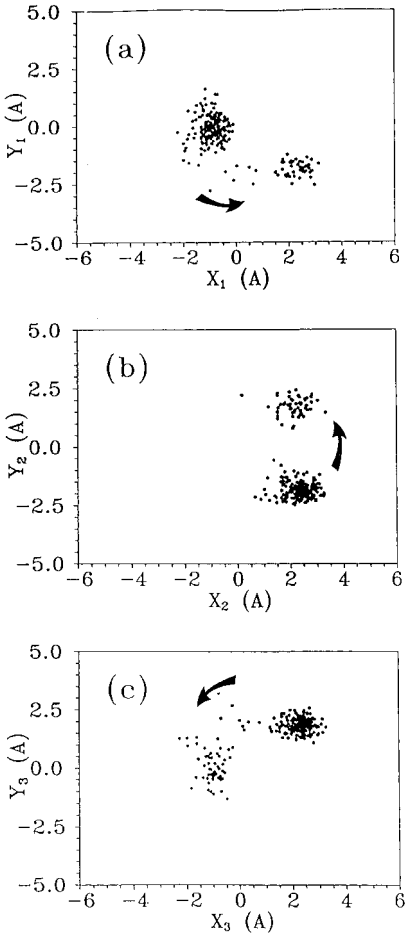

Figure 8. Clouds of points showing the successive positions of each (labeled) Ar atom in the case of the (3|0) isomer at $E = -1120$ cm^{-1} ($T = 17.6$K).

0.1),[44] reflecting a liquid-like behavior. However, the analysis of parameters such as λ_z, defined below in section 4.C.2 (eq 30), shows that no side-crossing transition appears in this range of energy. The large value of δ_{Ar-Ar} is in fact the consequence of an internal disorder of the trimer (*surface melting*). N. Ben-Horin et al.[57] have observed a similar behavior in the tetracene−Ar_3 cluster at $T = 15$ K. They associated it with the structural transformation between the triangular and linear conformations of the Ar_3 trimer already observed in simulations by Berry and co-workers[67] at $T = 18$ K. In the case of aniline−Ar_3, this transition appears at a higher temperature ($T = 38$ K). It is quite interesting to note that the changes of the transition temperature are in opposite directions when comparing tetracene−Ar_3 and aniline−Ar_3 to the neat Ar_3 cluster. The microsurface of tetracene, being a so-called "linear" polycyclic hydrocarbon, tends to make the triangular to linear transition easier by reducing the barrier height. On the contrary the trimeric configuration on the aniline microsurface involve larger barriers : only the "ring" atom is "supported" by the π-electronic cloud, the other two being sort of "separated" by the nitrogen $2p_z$-orbital repulsion.

The side-crossing transition is apparent when T becomes approximately equal to 54 K. This large value of the temperature reveals the fairly high stability of this (3|0) isomer and indicates that the isomerization barrier between the two distinct configurations (2|1) and (3|0) is rather high. This side-crossing transition appears at a higher temperature for the (3|0) isomer than for the (2|1) isomer (54 and 48 K), which simply reflects the difference in the binding energies of the two clusters.

In a previous experimental study of the electronic absorption spectra of the aniline−Ar_n clusters, Hermine et al.[9] have observed a net change in the aniline−Ar_3 spectral features as a function of the Ar partial pressure. When this partial pressure was increased, a progressive transfer of intensity from the (2|1) isomer bands to those of the (3|0) isomer was observed. One could question whether or not this observation is a signature of the isomerization transition.

From our numerical results, it seems very unlikely that an isomerization event between these two configurations can take place under the experimental conditions, because of the large value of the barrier height. Indeed, D. J. Wales[68] in a theoretical study, had also shown the quasi-impossibility to observe side-crossing transitions in typical experimental conditions. It seems more plausible that the pressure effect is the result of changes in the conditions of cluster formation in the supersonic jet. At high pressure, some large argon clusters may be preformed before they condense onto the aniline molecule. Consequently the collisional and/or evaporative cooling will preferably form asymmetric (3|0) clusters rather than the more symmetrical (2|1) isomers.

4.C. Aniline−Ar_n ($n = 4-6$). *4.C.1. Experimental and Theoretical Spectra.* While the electronic spectral shifts of the first three ($n = 1-3$) aniline−Ar_n clusters can be rationalized by the site specific modified shift additivity rule[9,14] on the basis of only two kinds of absorption sites (the *ring* site and the *-NH_2* site), a new type of site appears from $n = 4$ and above. It is then an opportunity to check for the predictive value of the spectral simulation method used throughout this article.

Figure 9 displays the geometrical configurations of the one-sided minimum energy structures obtained by the quenching technique for the clusters $n = 4$, 5, and 6. It should be noted

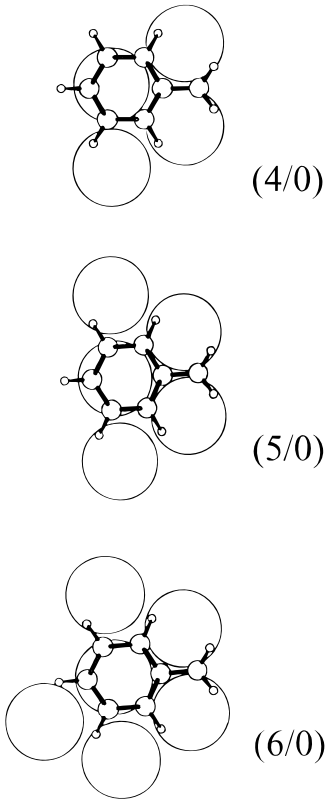

Figure 9. Calculated minimum energy structures for the one-sided isomers of aniline−Ar$_n$ ($n = 4-6$): (4|0), (5|0), and (6|0) . They involve one to three argon atoms bound in hydrogen sites.

that each of these (n|0) isomers corresponds to the most stable form of the cluster of size n. The (4|0) isomer has a structure very close to the (3|0) isomer with one extra argon atom interacting preferentially with peripheral hydrogen atoms. Such an adsorption site will be called a *hydrogen* site. It is of course of primary interest to assign it a *specific* electronic shift. The shifts of the other two isomers of $n = 4$ can be decomposed into known shifts of $n = 1-3$ clusters:

$$\Delta\nu(3|1) = \Delta\nu(3|0) + \Delta\nu(0|1)$$

$$\Delta\nu(2|2) = \Delta\nu(2|0) + \Delta\nu(0|2)$$

The $n = 5$ clusters may exist under three different isomeric forms, the most stable being the (5|0) isomer in which two argon atoms occupy equivalent hydrogen sites. Furthermore

$$\Delta\nu(4|1) = \Delta\nu(4|0) + \Delta\nu(0|1)$$

$$\Delta\nu(3|2) = \Delta\nu(3|0) + \Delta\nu(0|2)$$

The $n = 6$ clusters may exist under four different isomeric forms, the most stable being the (6|0) isomer in which three argon atoms occupy hydrogen sites. Furthermore

$$\Delta\nu(5|1) = \Delta\nu(5|0) + \Delta\nu(0|1)$$

$$\Delta\nu(4|2) = \Delta\nu(4|0) + \Delta\nu(0|2)$$

$$\Delta\nu(3|3) = \Delta\nu(3|0) + \Delta\nu(0|3)$$

These relations would permit filling in of the predicted electronic shifts appearing in the third column of Table 6, providing a value of the specific shift characterizing the hydrogen site is given.

TABLE 6: Electronic Shifts (in cm^{-1}) of the Various Structural Isomers of Aniline−Ar$_n$ Clusters ($n = 4-6$)

size	isomer	predicted from measurement	predicted from simulation	experiment
$n = 4$	(4|0)	−3.2	−3.4	−2.2
	(3|1)	−31.3	−37.2	−31.0
	(2|2)	−41.6	−45.8	not seen
$n = 5$	(5|0)	−26.3	−23.7	−25.5
	(4|1)	−55.4	*a*	−56.4
	(3|2)	+1.1	*a*	*+1.2*[b]
$n = 6$	(6|0)	−47.8	−43.1	−42.0
	(5|1)	−78.7	*a*	*a*
	(4|2)	−23.0	*a*	*−22.4*[b]
	(3|3)	+43.8	*a*	not seen

[a] Not evaluated. [b] Numbers in Italic Characters Correspond to tentative assignments.

At that point it is important to consider the outcome of the spectral simulation calculations, in order to compare with the experiment. The results are given in the fourth column of Table 6 for the three $n = 4$ isomers and for the one-sided (5|0) and (6|0) structures. The successive values of the hydrogen site shifts that can be deduced are

$$\Delta\nu_{sim}(4|0) - \Delta\nu_{sim}(3|0) = -3.4 - 14.8 = -18.2 \text{ cm}^{-1}$$

$$\Delta\nu_{sim}(5|0) - \Delta\nu_{sim}(4|0) = -23.7 - (-3.4) = -20.3 \text{ cm}^{-1}$$

$$\Delta\nu_{sim}(6|0) - \Delta\nu_{sim}(5|0) = -43.1 - (-23.7) = -19.4 \text{ cm}^{-1}$$

The fifth column of Table 6 contains the electronic shifts which have been derived from the new assignments to be made for the sizes $n = 4$, 5, and 6 and included in the new R2P2CI spectra of Figure 10. These spectra were recorded simultaneously (in a single scan) in experimental conditions close to those of Figure 3 but with a slightly longer delay between valve opening and laser firing.

The spectrum of the $n = 4$ clusters is extremely similar to the one in Figure 3. The assignment of the band at −31.0 cm^{-1} to the origin of the (3|1) isomer is clear from comparison with the values predicted by both the site specific shift additivity rule (column 3) and the simulation method (column 4) in Table 6. The spectrum of the $n = 5$ clusters also exhibits a rich set of narrow bands. The band at −56.4 cm^{-1} appears as the origin of a transition from the global pattern of the spectrum. The only structural isomer expected to absorb to the red of the (3|1) origin is the (4|1) structure. Its assignment is fully consistent with that of the (4|0) isomer at −2.2 cm^{-1}, in fair agreement with the prediction from the spectral simulation. It leads to an experimental value of the hydrogen site specific shift of $\Delta\nu_{exptl}(4|0) - \Delta\nu_{exptl}(3|0) = -2.2 - 21.9 = -24.1$ cm^{-1}, in good agreement with that derived from the simulation (see above). The red character of this shift shows that the system is stabilized upon excitation (vdW interaction stronger in S_1 than in S_0) for an Ar atom located in a *hydrogen* site. In the benzene−Ar$_n$ cluster, it has been experimentally observed[29] that the presence of argon atoms in a similar site produces a small effect in the opposite direction (associated electronic shift +3 cm^{-1}). This difference of behavior can be explained by the presence of the $-NH_2$ group and of a strong charge transfer between the nitrogen atom and the phenyl ring induced by the optical $S_1 \leftarrow S_0$ excitation of the aniline molecule. As mentioned before, this same explanation accounts for the strong stabilization of the cluster in the first excited state when the

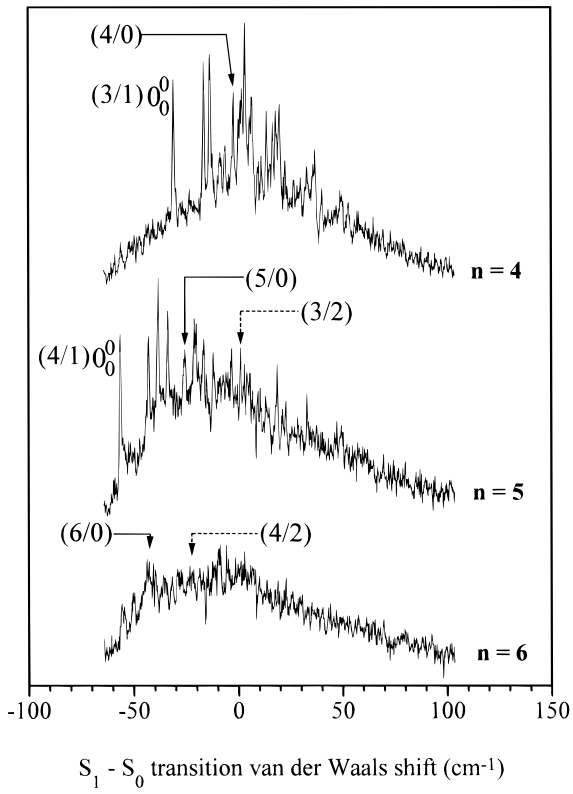

Figure 10. Experimental R2P2CI spectra of the aniline−Ar_n clusters ($n = 4-6$) taken with 1% Ar/He gas mixture expanded from stagnation pressure $P_0 = 5$ bar. Only the origins of the identified structural isomers are labeled. Many excited vdW bands are visible for $n = 4$ and 5. The dotted arrows indicate tentative assignments. The frequency scale refers to the origin of the monomer 0_0^0 band.

solvent atoms are located in the main site (ring). The position of the (5|0) isomer origin band is obtained by using

$$\Delta\nu_{exptl}(5|0) = \Delta\nu_{exptl}(4|0) + [\Delta\nu_{exptl}(4|0) - \Delta\nu_{exptl}(3|0)] = -26.3\ cm^{-1}$$

which permits assignment of it to the band experimentally found at -25.5 cm^{-1}. The position predicted by the spectral simulation being -23.7 cm^{-1}, a very good agreement is again found between theory and experiment. The third $n = 5$ isomer, the (3|2) structure, expected at $+1.1$ cm^{-1}, can tentitatively find an assignment at $+1.2$ cm^{-1}. It can be noted that the assignment of origin bands which can lie very close in frequency to vdW excited bands of other isomers is really difficult. Indeed we previously assigned[61] the band at -2.4 cm^{-1} (origin of the (4|0)) to the $sh_x^2 0$ band of the (3|1) isomer. Hole-burning or ionization-selective experiments[12] would help to confirm such assignments (accidental superimposition is also possible). The spectrum of the $n = 6$ clusters shows less resolution. Nonetheless tentative assignments can be done for the (6|0) isomer at -42.0 cm^{-1} and the (4|2) at -22.4 cm^{-1}. It is worth noting that the (n − 2|2) isomers which have been found less secure to identify in the spectra correspond to structural configurations which are less stable than the corresponding (n|0) configurations by about 70 cm^{-1}. At the same time it seems that the (n − 1|1) clusters are favored in the formation process; they could be the combined result of binding a preformed cluster and a single atom on both sides of the substrate.

From the above discussion on spectral assignments the capability of the spectral simulation method at reproducing shifts seems to be outstanding. One may interrogate now about its ability to reproduce widths.

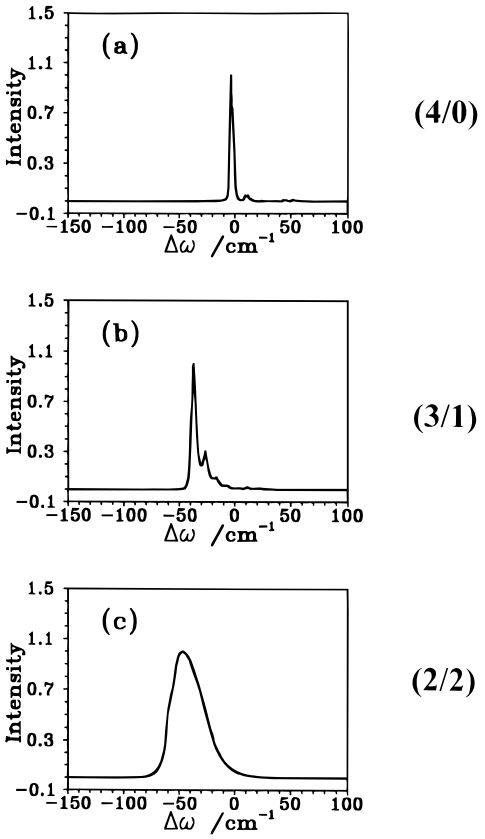

Figure 11. Simulated spectra of the three $n = 4$ isomeric clusters at $T = 5$ K: (a) (4|0); (b) (3|1); (c) (2|2).

The theoretical electronic spectra simulated at $T = 5$ K for the three configurations of $n = 4$ clusters which are, by order of decreasing stability, (4|0), (3|1), and (2|2), obtained by averaging over 25 subspectra are displayed in Figure 11. The shifts and vdW frequencies have been already discussed above (see Table 6). Although vdW bands appear in the spectra of the (4|0) and (3|1) isomers, no similar structure is visible in the broad (2|2) isomer spectrum.

The large differences (especially in broadening) between the different isomers of aniline−Ar_4 call out for an analysis based on the Δ parameter in order to correlate the spectra with the underlying dynamics. Thus, the value of Δ (see eq 28) was calculated for each subspectrum of the three different isomers. Although the various Δ values were found very close to one another for the (4|0) isomers and (3|1) isomers (with slightly larger values for the (3|1) isomer), Δ exhibits much larger values in the case of the (2|2) isomer. For each isomer, the mean value of Δ (on the different subspectra) approximately correlates with the fwhm, W, of the simulated spectrum. Indeed we found $\langle\Delta\rangle_{(4|0)} = 19.75$, $\langle\Delta\rangle_{(3|1)} = 20.88$, and $\langle\Delta\rangle_{(2|2)} = 29.35$ cm^{-1}, to be compared with $W_{(4|0)} = 3.8$, $W_{(3|1)} = 5.3$, and $W_{(2|2)} = 34.9$ cm^{-1}. But the spectral width of each subspectrum is not directly connected to the corresponding value of Δ. Moreover, the ratio of the spectral width to Δ is clearly larger for the (2|2) isomer.

As already noted by Fried and Mukamel[58] in the case of benzene−Ar_n, the fwhm of the simulated spectra is always found to be lower than 2.35Δ in this range of size and temperature. Consequently, it does not seem rational to deduce the fwhm of the electronic spectra for the small size vdW clusters at these temperatures by only using the proportionality relationship (eq 29). In fact, Fried and Mukamel[58] have shown that this criterion could be used for the large clusters where a static regime is

attained. The results in our case show that the small clusters are not in the static regime.

Furthermore we checked whether the noticeable broadening appearing in the (2|2) isomer was homogeneous or not. For that purpose the spectral shift was calculated for each individual subspectrum of each isomer. In the case of the (4|0) and (3|1) isomers, the spectral shifts $\Delta\nu_i$ showed little dispersion, being well grouped around their mean value ($-6.1\ \text{cm}^{-1} < \Delta\nu_{i,(4|0)} < -1.0\ \text{cm}^{-1}$ and $-40.3\ \text{cm}^{-1} < \Delta\nu_{i,(3|1)} < -35.1\ \text{cm}^{-1}$). This reflects the fact that these two isomers only vibrate around their respective equilibrium positions without making transitions to other isomeric configurations.

On the other hand, the dynamical behavior of the (2|2) isomer was found to be quite different. The distribution of spectral shifts is spread out from -60.9 to $-28.1\ \text{cm}^{-1}$. Simultaneously, the fwhm of individual subspectra are of the same order of magnitude as the dispersion of the spectral shifts. We conclude then that the observed broadening for the (2|2) isomer is due to both homogeneous and inhomogeneous contributions. As in the case of the (2|0) isomer, it is difficult to distinguish between the two contributions since they are strongly linked: for a surface transition involving different isomeric conformations, the solvent induced perturbation of the chromophore electronic transition strongly depends on the localization of the Ar atoms.

The analysis of the trajectories revealed that, at $T = 5$ K, the Ar_2 dimer (being on the same side as the $-NH_2$ group hydrogen atoms) displays a windscreen wiper motion as in the (2|0) isomer.[27] In the case of the (2|2) isomer, this motion appears at an even lower temperature because the isomerization barrier (racemization) is lower for the dimer which is located on the side of the two (out of plane) substituent hydrogen atoms. To confirm this assumption, the electronic spectrum was simulated at $T = 2.5$ K, and a structured spectrum was found reflecting the rigidity of this cluster at this very low temperature. This theoretical finding provides a plausible explanation for the *absence of any experimental evidence* for spectral features which could be assigned to the (2|2) isomer.

A final question might be addressed after careful examination of the $n = 4-6$ experimental spectra in Figure 10. The narrow bands, which can be assigned to the origin or to vdW excited bands of the various identified structural isomers, appear as superimposed on a broad background. The origin of this background is not completely clear at present time. Among other hypotheses, the possible existence of a bimodal distribution of cluster temperatures is being considered. Numerical investigations of the solid-like to liquid-like phase transition have revealed that it requires temperatures of the order of 35 K. Preliminary investigations of the evaporation processes[69] show that the temperatures which could be attained by evaporative cooling in our experimental conditions are of the order of 45 K in this range of sizes. This last temperature being above the phase transition, it would explain the broad band character of "liquid" clusters.

In the conclusion of this section it is worth noting that both the strong specificity of the electronic shift and the large Franck−Condon activity of excited vdW modes appear to be a typical character for the clusters in which the aniline molecule is the chromophore, contrary to the more symmetrical chromophores like benzene,[29] naphthalene,[6] and 9,10-dichloroanthracene.[7] Note that similar interesting behaviors have recently been found in the vdW clusters of 4-fluorostyrene with argon[70] and had also been noted for the cases of phenylacetylene[4] and *p*-xylene.[10] Thus this character seems to be associated to substituted benzene chromophore. Naturally resulting from these characteristics is an increased sensitivity of the spectra to the dynamics of the solvent atoms as already mentioned. On the contrary it is highly probable that the spectral simulations performed on tetracene−Ar_n[64] could not reveal any surface transitions because of the weak specificity of the shifts in that system.

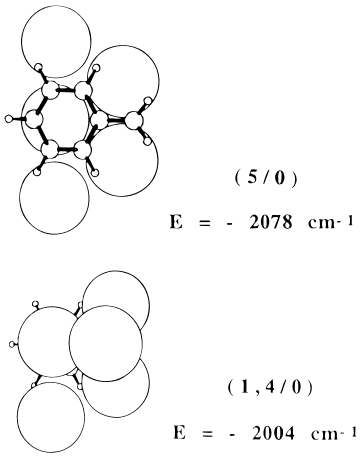

Figure 12. Calculated minimum energy structures for the (5|0) and (1,4|0) isomers of aniline−Ar_5.

4.C.2. Isomerization Dynamics for Aniline−Ar_5 [(1,4|0) and (5|0) Isomers]. Before coming to a general conclusion of this study of the small sizes of aniline−Ar_n clusters, we focus in this subsection mainly on the *wetting−nonwetting* transition which connects multilayer argon cluster structures with planar configurations that retain all atoms on the same side of the phenyl ring. Indeed the aniline−Ar_5 cluster is one of the smallest system where some *multilayer* structures are present. Further manifestations of wetting are observed in larger clusters which will be described in paper 2.

We have undertaken a study of the isomerization processes that can occur in aniline−Ar_5 starting from both the metastable (1,4|0) isomer ($E = -2004\ \text{cm}^{-1}$) and the more stable (5|0) isomer ($E = -2078\ \text{cm}^{-1}$). Both systems have been studied using trajectories of 1.5 ns duration at a variety of increasing energies. The two involved structures are shown in Figure 12. These isomerization transitions have been identified by analyzing additional parameters generated during the MD trajectories. The first of these is defined as follows

$$\lambda_y = \sum_{i=1}^{n} y_i \tag{30}$$

where the y_i are the coordinates of the argon atoms along the short inertial axis of the aniline molecule. Positive (negative) values of λ_y imply more (fewer) atoms on a given side of the σ_v symmetry plane. A second set of parameters measures the relative mobility of each (labeled) argon atom relative to aniline

$$\sigma_i = \frac{\sqrt{\langle d_i^2\rangle - \langle d_i\rangle^2}}{\langle d_i\rangle} \tag{31}$$

where d_i is the distance between atom i and the center of mass of the aniline molecule.

Several distinct structural transitions appeared, as a function of the internal energy, for the (1,4|0) isomer which can be summarized as follows.

Surface Transition: it appears at approximately $E = -1917\ \text{cm}^{-1}$ ($T = 8$ K). Only two Ar atoms of the first solvation layer are involved in this transition. These two atoms begin to cross

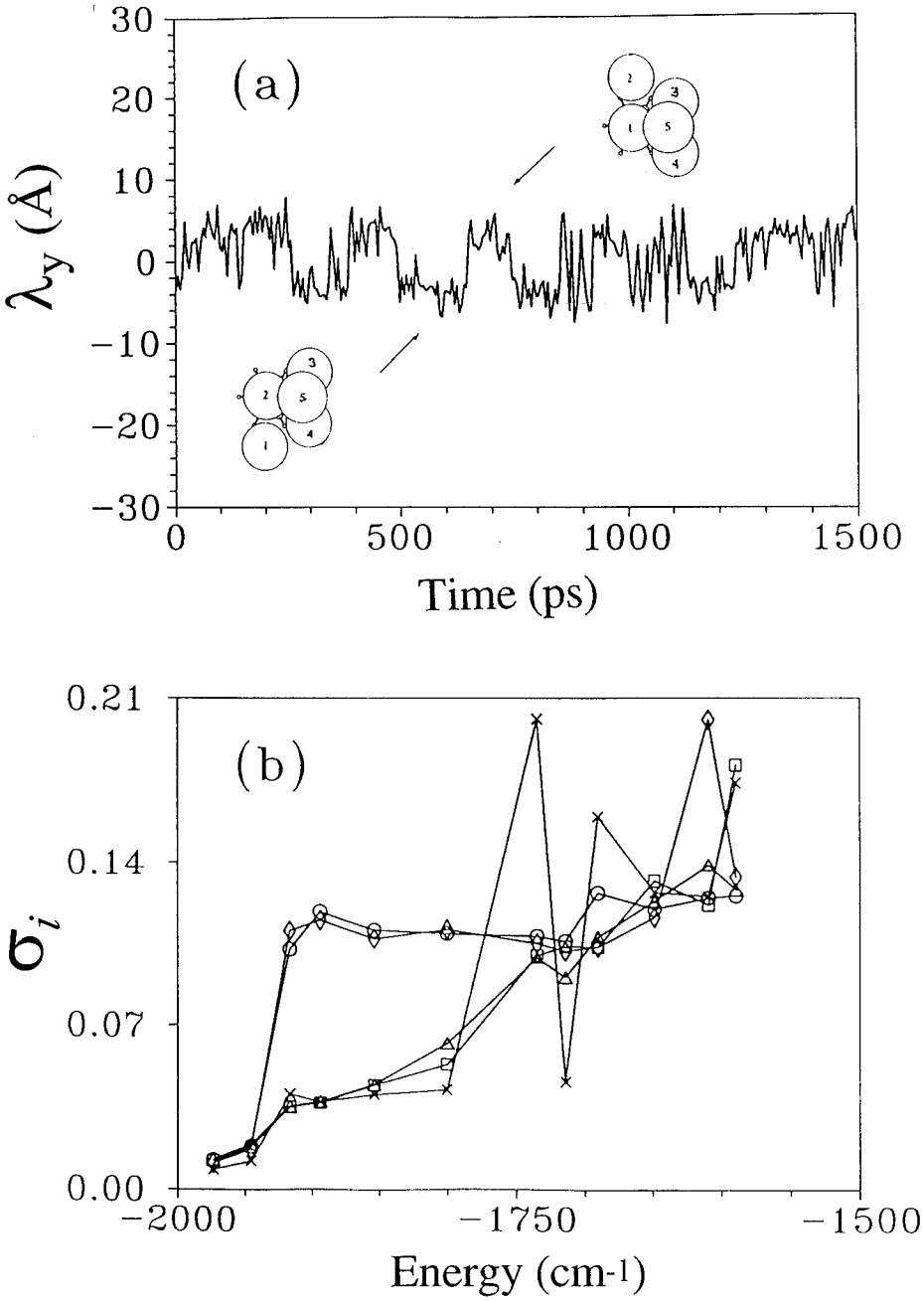

Figure 13. (a) Evolution of λ_y as a function of time for the (1,4|0) isomer (simulation at $T = 13.5$ K). (b) Relative mean square values (σ) for the distance of each Ar atom i to the aniline center of mass in the (1,4|0) isomer versus total energy. Symbols (○ atom 1; ◊ atom 2; △ atom 3; □ atom 4; × atom 5) refer to the labeling of the atoms shown in panel a.

the $y = 0$ plane and move between the two equivalent configurations as in the case of the (2|0) and (2|1) isomers. This specific dynamics can be easily observed by looking at the time evolution of the λ_y parameter along a typical microcanonical trajectory, such as that shown in Figure 13a for a 1.5 ns trajectory at $T = 13.5$ K. This observable λ_y oscillates between -3 and $+3$ Å. The two structures, corresponding to these two extreme values, are indicated in the same graph. In this range of temperatures, the Ar atom being located in the second solvation layer, is always strongly rigid (its corresponding σ value being weak as we can note in Figure 13b). As a consequence the system only evolves between these two equivalent symmetric structures with respect to the $y = 0$ plane. The analysis of the evolution of all the σ parameters for each Ar atom (Figure 13b) shows that only two of these parameters (σ_1 and σ_2) are affected from $T = 8$ K, confirming the previously proposed dynamical scheme.

3D−2D Transition: from $T = 25$ K and above, the Ar atom located in the second solvation layer begins to communicate with the first layer (strong increase of σ_5), thus forming (5|0) isomers. This transition appears when the structure formed by the four Ar atoms in the first layer is already strongly altered. It is indeed allowed by the melting of the first layer revealed by a high value of δ_{Ar-Ar}. This transition seems to be quasi-irreversible: a very small fraction of the trajectories have allowed observation of a comeback to a two-layer structure. This nonreversibility has also recently been observed by M. Schmidt et al.[29] in a Monte-Carlo simulation study of the benzene−Ar_5 cluster.

Side-crossing transition: the (5|0), (4|1), and (3|2) isomers begin to comunicate at $T \cong 36$ K. From this temperature, many structural forms are energetically accessible. However the two-layer structures are hardly observed during the microcanonical dynamics. This finding could be important when considering

the relative populations of various isomers during the clustering processes in a supersonic jet.

The situation is simpler when the trajectories are initiated in the most stable one-sided (5|0) isomer. A first surface transition is observed at about $E = -1835$ cm^{-1} ($T = 20$ K), for which the δ_{An-Ar} and δ_{Ar-Ar} parameters sharply increases together at the same internal energy. This feature is explained by the apparition of a global decoupling of a nonrigid Ar_5 cluster at this energy. The surface transition takes place in the plane parallel to the aniline molecule putting the different (5|0) structural forms into communication, as shown by observation of the mean kinetic energy and of the λ_y parameter versus time. This transition is naturally associated with an increased fluxionality within the planar argon cluster. At slightly higher energy, a *surface fusion* (total disorganization of the Ar atoms in the plane parallel to the substrate) is observed, indicated by larger values of the δ_{Ar-Ar} parameter. In this range of energy, it becomes difficult to distinguish different structural configurations inside the given family of (5|0) isomers.

When the internal energy of the cluster is further increased, a side-crossing transition is finally taking place around $T = 33$ K. It is interesting to note that in all the trajectories initiated in the (5|0) family of isomers, we never observed the appearance of any (1,4|0) structures, which confirms the quasi-irreversible character of the (1,4|0) → (5|0) isomerization process.

5. Conclusion

The present paper (1) devoted to the discussion of R2P2CI spectra of size and isomer selected VdW clusters associating one to six argon atom(s) to the aniline molecule as a chromophore has brought a consistent picture of the first steps of the solvation process, wich will be used as a background for the study of the further steps of the same process, when the cluster size grows from 7 to 25 solvent atoms (paper 2). It has revealed in particular the major role played by the structural constraints in the cluster growth.

In the body of this article a coherent presentation of both experimental *and* theoretical results is given, including the results of spectral simulations by MD techniques for every cluster size. Good agreement between experimental and simulated spectra was obtained for numerous isomers absorbing in the vicinity of the 0_0^0 band origin of the aniline molecule.

On the one hand, this proves the reality of the previously proposed modified spectral shift additivity rule making use of the site specificity. Indeed the electronic shift induced by the binding of argon atoms was found to be strongly dependent on the localization of the atoms with respect to the aniline substrate. This strong electronic effect is a direct consequence of the substitution of one hydrogen atom (in benzene) by the amino $-NH_2$ group. It was introduced in the theoretical approach by an adequate empirical term in the potential energy surface, accounting for the specific role played by the lone pair orbital on nitrogen atom when the aniline molecule is electronically excited.

On the other hand, the spectral simulations have proven to be predictive in their ability to provide the electronic shifts for structural isomers which were not yet experimentally characterized. In particular an individual red shift of about -20 cm^{-1} has been predicted for an argon atom located near the hydrogen atoms of the aromatic ring, which was confirmed by experimental findings in clusters binding four to six argon atoms.

Extensive use has been made of the MD simulations to investigate the dynamical effects to be observed in well-defined selected structural isomers. For the (2|0) isomer, a net temperature effect was seen in the spectral widths, which appears as controlled by the dynamical behavior with the onset of new large amplitude motions. The dynamics of isomerization transitions in aniline−Ar_3 and aniline−Ar_5 has also been explored, and their consequences have been discussed in relation to experiment.

The predictive character of the simulation techniques will be further exploited in the interpretation of the R2PI spectra of larger clusters ($n = 7-25$), which is the subject of paper 2.

Acknowledgment. Support from the NATO Collaborative Research Grants program (CRG 920289) is gratefully acknowledged. The authors also thank the referee for his very careful reading which helped in the improvement of the manuscript.

References and Notes

(1) Leutwyler, S.; Jortner, J. *J. Phys. Chem.* **1987**, *91*, 5558.
(2) Leutwyler, S.; Bösiger, J. *Chem. Rev.* **1990**, *90*, 489.
(3) Menapace, J. A.; Bernstein, E. R. *J. Chem. Phys.* **1987**, *91*, 2533.
(4) Dao, P. D.; Morgan, S.; Castleman, A. W. *Chem. Phys. Lett.* **1984**, *111*, 38.
(5) Weber, Th.; von Bargen, A.; Riedle, E.; Neusser, H. J. *J. Chem. Phys*. **1990**, *92*, 90.
(6) Troxler, T.; Leutwyler, S. *J. Chem. Phys*. **1991**, *95*, 4010.
(7) Even, U.; Ben-Horin, N.; Jortner, J. *Chem. Phys. Lett*. **1989**, *156*, 138. Ben-Horin, N.; Bahatt, D.; Even, U.; Jortner, J. *J. Chem. Phys*. **1992**, *97*, 6011.
(8) Mandziuk, M.; Bacic, Z.; Droz, T.; Leutwyler, S. *J. Chem. Phys*. **1994**, *100*, 52.
(9) Hermine, P.; Parneix, P.; Coutant, B.; Amar, F. G.; Bréchignac, Ph. *Z. Phys. D*: At., Mol. Clusters **1992**, *22*, 529.
(10) Dao, P. D.; Morgan, S.; Castelman, A. W., Jr. *Chem. Phys. Lett*. **1985**, *113*, 219.
(11) Shchuka, M.; Motyka, A. L.; Topp, M. R. *Chem. Phys. Lett*. **1989**, *164*, 87.
(12) Knochenmuss, R.; Leutwyler, S. *J. Chem. Phys*. **1990**, *92*, 4686.
(13) Schmidt, M.; Mons, M.; Le Calvé, J. *J. Phys. Chem*. **1992**, *96*, 2404.
(14) Douin, S.; Hermine, P.; Parneix, P.; Bréchignac, Ph. *J. Chem. Phys.* **1992**, *97*, 2160.
(15) Troxler, T.; Knochenmuss, R.; Leutwyler, S. *Chem. Phys. Lett*. **1989**, *159*, 554.
(16) Schmidt, M.; Mons, M.; Le Calvé, J. *Chem. Phys. Lett*. **1991**, *177*, 371.
(17) Ben-Horin, N.; Even, U.; Jortner, J. *J. Chem. Phys*. **1992**, *97*, 5988.
(18) Brocks, G.; Huygen, T. *J. Chem. Phys.* **1986**, *85*, 3411. Brocks, G.; Van Koeven, T. *Mol. Phys*. **1988**, *63*, 999.
(19) Tiller, A. R.; Clary, D. C. *J. Chem. Phys.* **1990**, *92*, 5875.
(20) Bludsky, O.; Spirko, V.; Hrouda, V.; Hobza, P. *Chem. Phys. Lett.* **1992**, *196*, 410.
(21) Van der Avoird, A. *J. Chem. Phys*. **1993**, *98*, 5327.
(22) Mandziuk, M.; Bacic, Z. *J. Chem. Phys*. **1993**, *98*, 7165.
(23) Parneix, P.; Halberstadt, N.; Bréchignac, Ph.; Amar, F. G.; van der Avoird, A.; van Bladel, J. W. I. *J. Chem. Phys.* **1993**, *98*, 2709.
(24) Vacek, J.; Konvicka, K.; Hobza, P. *Chem. Phys. Lett*. **1994**, *220*, 85. Vacek, J.; Hobza, P. *J. Phys. Chem.* **1994**, *98*, 11034.
(25) Ben-Horin, N.; Even, U.; Jortner, J. *Chem. Phys. Lett*. **1992**, *188*, 73.
(26) Heidenreich, A.; Bahatt, D.; Ben-Horin, N.; Even, U.; Jortner, J. *J. Chem. Phys.* **1994**, *100*, 6300.
(27) Parneix, P.; Amar, F. G.; Bréchignac, Ph. *J. Chem. Phys.* **1996**, *104*, 983.
(28) Adams, J. E.; Stratt, R. M. *J. Chem. Phys*. **1990**, *93*, 1358.
(29) Schmidt, M.; Le Calvé, J.; Mons, M. *J. Chem. Phys*. **1993**, *98*, 6102.
(30) Bösiger, J.; Bombach, R.; Leutwyler, S. *J. Chem. Phys*. **1991**, *94*, 5098.
(31) Hobza, P.; Selzle, H. L.; Schlag, E. W. *J. Chem. Phys.* **1991**, *95*, 391.
(32) Boesiger, J.; Knochenmuss, R.; Leutwyler, S. *Phys. Rev. Lett*. **1989**, *62*, 3058.
(33) Boesiger, J.; Leutwyler, S. *Phys. Rev. Lett*. **1987**, *59*, 1895.
(34) Douin, S.; Fillion, J. H.; Bonneau, M.; Bréchignac, Ph.; Furio, D.; Gauyacq, D.; Horani, M.; Shafizadeh, N. *Chem. Phys. Lett*. **1993**, *216*, 215.
(35) Kruit, P.; Read, F. H. *J. Phys. E: Sci. Instrum*. **1983**, *16*, 313.
(36) vans, D. J. *Mol. Phys.* **1977**, *34*, 317. Evans, D. J.; Murad, S. *Mol. Phys.* **1977**, *34*, 327.
(37) Lombardi, J. R. *J. Chem. Phys.* **1969**, *50*, 3780.
(38) Jackson, J. D. *Classical Electrodynamics*; Wiley: New York, 1962.
(39) Aziz, R. A.; Chen, H. H. *J. Chem. Phys*. **1977**, *67*, 5719.
(40) Weerasinghe, S.; Amar, F. G. Unpublished work.

(41) Kaelberer, J. B.; Etters, R. D. *J. Phys. Chem.* **1977**, *66*, 3233.
(42) Jellinek, J.; Beck, T.; Berry, R. S. *J. Chem. Phys.* **1986**, *84*, 2783.
(43) Amar, F. G.; Berry, R. S. *J. Chem. Phys.* **1986**, *85*, 5943.
(44) Kaelberer, J. B.; Etters, R. D. *J. Phys. Chem.* **1977**, *66*, 3233.
(45) Lax, M. *J. Chem. Phys.* **1952**, *20*, 1752.
(46) Evans, M.; Evans, G. J.; Coffey, W. T.; Grigolini, P. *Molecular Dynamics*; Wiley: New York, 1982.
(47) Bratos, S. *Vibrational spectroscopy of Molecular liquids and solids*; Plenum: New York, 1980; p 43.
(48) Mukamel, S. *Phys. Rep.* **1982**, *93*, 1. Mukamel, S. *Phys. Rev. A.* **1982**, *26*, 617.
(49) Breene, R. G., Jr. *Theories of spectral line shapes*; Wiley: New York, 1981.
(50) Islampour, R.; Mukamel, S. *J. Chem. Phys.* **1984**, *80*, 5487. Islampour, R.; Mukamel, S. *Chem. Phys. Lett.* **1984**, *107*, 2391.
(51) Warshel, A.; Stern, P. S.; Mukamel, S. *J. Chem. Phys.* **1983**, *78*, 7498.
(52) Mukamel, S. *J. Chem. Phys.* **1982**, *77*, 173.
(53) Berne, B. J.; Harp, G. D. *Adv. Chem. Phys.* **1970**, *17*, 63.
(54) Nosé, S. *Mol. Phys.* **1984**, *52*, 255. Nosé, S. *J. Chem. Phys.* **1984**, *81*, 511. Nosé, S.; Yonezawa, F. *J. Chem. Phys.* **1984**, *84*, 1803.
(55) Generally used in such problems and defined by

$$F(t) = A_0 - A_1 \cos(2\pi t/T) + A_2 \cos(4\pi t/T) - A_3 \cos(6\pi t/T)$$

with $A_0 = 0.40217$, $A_1 = 0.49703$, $A_2 = 0.09392$, and $A_3 = 0.00183$. T is the total duration of the trajectory ($T = 107.46$ ps). Press, W. H.; Flannery, B. P.; Teukolsky, S. A.; Vettering, W. T. *Numerical recipes: The Art of Scientific Computing*; Cambridge University Press, Cambridge, 1986.
(56) Kubo, R.; Toyozawa, Y. *Prog. Theor. Phys.* **1955**, *13*, 160.
(57) Ben-Horin, N.; Even, U.; Jortner, J.; Leutwyler, S. *J. Chem. Phys.* **1992**, *97*, 5296.
(58) Fried, L. E.; Mukamel, S. *Phys. Rev. Lett.* **1991**, *66*, 2340. Fried, L. E.; Mukamel, S. *J. Chem. Phys.* **1992**, *96*, 116.
(59) Bieske, E. J.; Uichanco, A. S.; Rainbird, M. M.; Knight, A. E. W. *J. Chem. Phys.* **1991**, *94*, 7029.
(60) Maxton, P. M.; Schaeffer, M. W.; Ohline, S. M.; Kim, W.; Venturo, V. A.; Felker, P. M. *J. Chem. Phys.* **1994**, *101*, 8391.
(61) Douin, S.; Bréchignac, Ph. *J. Chim. Phys.* **1995**, *92*, 283.
(62) Douin, S.; Piccirillo, S.; Bréchignac, Ph., in preparation.
(63) Schmidt, M.; Mons, M.; Le Calvé, J. *Z. Phys. D. At., Mol. Clusters* **1990**, *17*, 153.
(64) Heidenreich, A.; Jortner, J. *Z. Phys. D At., Mol. Clusters* **1993**, *26*, 377.
(65) Crépin, C.; Tramer, A. *Chem. Phys. Lett.* **1990**, *170*, 446.
(66) Gutmann, M.; Schonzart, P. F.; Hohlneicher, G. *Chem. Phys.* **1990**, *140*, 107.
(67) Beck, T. L.; Leitner, D. M.; Berry, R. S. *J. Chem. Phys.* **1988**, *89*, 1681. Leitner, D. M.; Berry, R. S.; Whitnell, R. M. *J. Chem. Phys.* **1989**, *91*, 3470.
(68) Wales, D. J. *Mol. Phys.* **1991**, *74*, 1.
(69) Parneix, P.; Bréchignac, Ph. Work in progress.
(70) Piccirillo, S.; Consalvo, D.; Coreno, M.; Giardini-Guidoni, A.; Douin, S.; Parneix, P.; Bréchignac, Ph. *Chem. Phys.* **1994**, *187*, 97.